UILU-ENG-86-2550

DYNAMIC PERFORMANCE OF SYNCHRONOUS MACHINES WITH UNDEREXCITATION LIMITERS

ABRAHAM VARGHESE

Power Affiliates Program

Department of Electrical and Computer Engineering

University of Illinois at Urbana-Champaign

Urbana, Illinois 61801

PAP-TR-85-5

October, 1985

FOREWORD

This technical report is a reprint of the thesis written by Mr. Abraham Varghese as partial fulfillment of the requirements for the degree of Master of Science in Electrical Engineering at the University of Illinois. His research was supported in part through the Power Affiliates Program, and in part by National Science Foundation Grant NSF ECS 84-14677.

P. W. Sauer
Thesis Advisor
October 1985

TABLE OF CONTENTS

LIST OF TABLES

LIST OF FIGURES

1. INTRODUCTION

1.1. Motivation

Power requirements for consumers, including industrial requirements, historically have doubled every ten years. This increased development of power systems in size as well as complexity calls for improved methods of controlling power system electrical quantities. System stability, determined by the real and reactive power values at various points, becomes more and more important as systems grow larger.

Essentially, power system operation consists of generators delivering a certain real power P to a group of loads, at some specified terminal voltage E_t. The turbine-governor subsystem ensures the delivery of sufficient shaft power to the generator to supply P. Alongside, the regulator-exciter subsystem maintains the generator terminal voltage at the specified value E_t. As a consequence of external conditions, there exists in the system an additional quantity - Q, the reactive power.

Being a physical system, there are various restrictions on the amount of P and Q a generator can supply. The limiting values are given by "capability curves" of generators. A typical curve is shown in Figure 1.1 [1]. Thermal limitations on different windings account for the entire curve. Heating limitations on the field cause AB, while armature winding thermal limits restrict operation to BC. The portion CD limits generator operation in the underexcited mode, and is determined by thermal limits imposed on the stationary end structure parts of the machine.

So long as all the controls associated with the generator function properly, the region of safe operation remains the one specified by capability curves. But to ensure full reliability, it is necessary to check for further

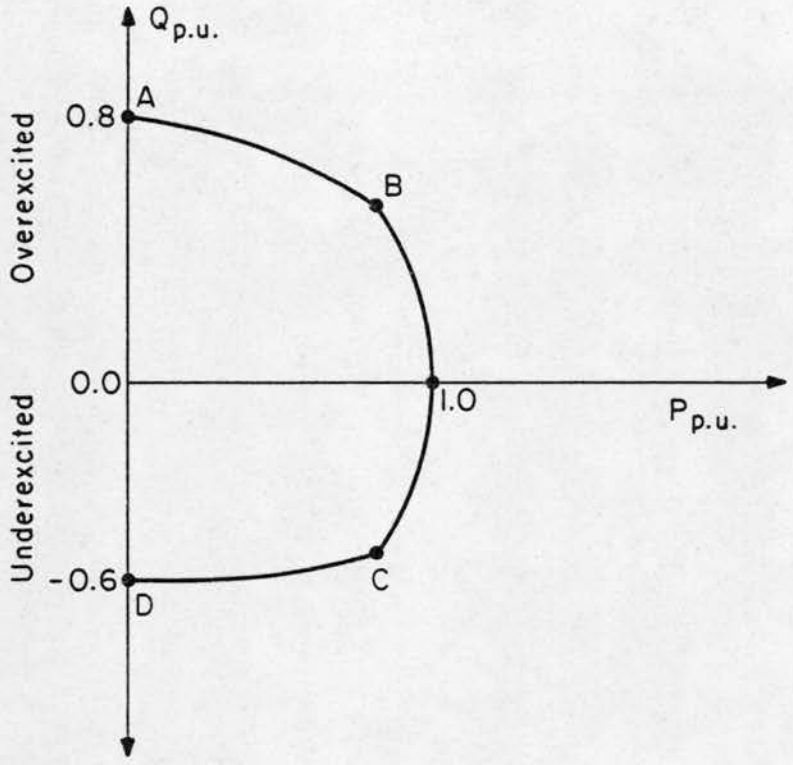

Figure 1.1. A generator capability curve.

restrictions on this region in case of failure of one or more controls. An important additional limitation that may come in is the Steady-State Stability Limit (SSSL) of the generator in the absence of a regulator. This is illustrated in Figure 1.2 (curve A) along with the capability curve. (The location of this curve varies depending on the machine and system constants and the terminal voltage of the machine.) Curve B is the SSSL when the regulator is in operation.

Hence, it is necessary to make sure that even during normal operation, the machine excitation does not go below the SSSL without a regulator. This is achieved using an Underexcitation Limiter (UEL), whose characteristic is given by curve A' in Figure 1.2.

As explained above, the UEL setting is based on the SSSL curve of the generator. Most of the existing literature on steady state stability of machines

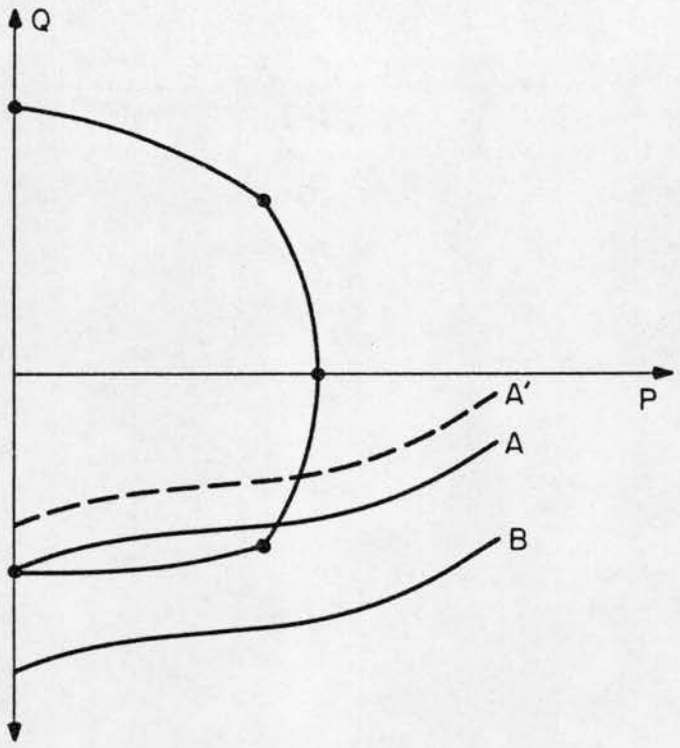

Figure 1.2. Steady-state stability limits of a generator.

is based on work done decades ago using models and techniques which are heuristic in origin. Hence, it was felt that a reexamination of steady-state stability criteria used today would be of interest, with the aid of precise models and exact methods of analysis. The first part of this work derives the exact conditions for steady-state stability (without regulator) of a synchronous machine in a single machine-infinite bus system.

The second part deals with the UEL itself. It was found necessary to study the UEL in detail, since modern literature does not give a good idea about this vital component of the generator protection system. In this work, parameters relevant to UEL performance are identified by analyzing its behavior during relevant contingencies.

1.2. Literature Summary

1.2.1. Steady-state stability

Steady-state stability is the ability of a synchronous machine to remain in synchronism after small disturbances such as gradual load changes, changes in excitation, etc. SSSL refers to the maximum power that can be transmitted on a specified circuit, under specified operating conditions, without the loss of synchronism [2]. Traditionally, power angle curves have been the basis for determining steady-state stability. Consider the two-machine system of Figure 1.3.

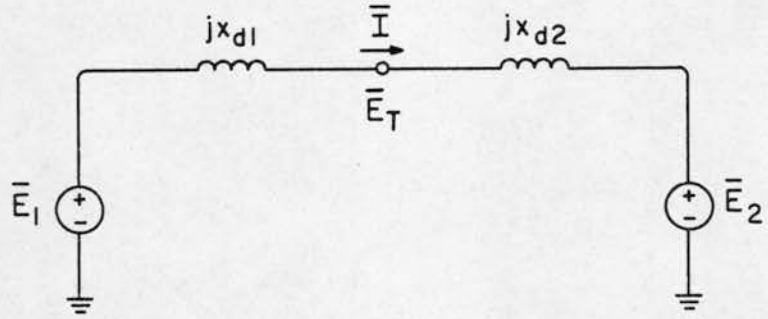

Figure 1.3. Two-machine system.

Both are assumed round rotor, and are represented by internal voltages behind equivalent synchronous reactances, with constant field excitation. The power transferred from $\overline{E}_1$ to $\overline{E}_2$ is given by

$$P = \frac{|\overline{E}_1||\overline{E}_2|}{(x_{d1} + x_{d2})} \sin \delta \qquad (1.1)$$

where δ is the angle by which $\overline{E}_1$ leads $\overline{E}_2$, or the angle of separation of the two rotors. Since $|\overline{E}_1|$ and $|\overline{E}_2|$ are both proportional to the excitation current, they remain constant for fixed excitation current. Equation (1.1) represents the power angle curve of the above system.

Under fixed excitation, the maximum value of P occurs at $\delta = 90°$,

$$P_m = \frac{|\overline{E}_1||\overline{E}_2|}{(x_{d1} + x_{d2})} \tag{1.2}$$

Since this point corresponds to the peak of a sine curve, (P vs. δ) it is argued that any attempt to increase δ beyond 90° leads to conditions amounting to positive feedback, and hence, synchronism will be lost. This resulted in $\delta = 90°$ being accepted as the stability limit.

The current in the system is

$$\overline{I} = (\overline{E}_1 - \overline{E}_T)/j\, x_{d1} \tag{1.3}$$

and the transferred power is

$$\overline{S} = P + jQ = \overline{E}_T\, \overline{I}^* \tag{1.4}$$

where $\overline{I}^*$ is the complex conjugate of $\overline{I}$.

Assuming the second machine to be an infinite bus along with an equivalent system reactance x_e, Adams and McClure [3] have shown that Equation (1.3) can be modified to give the equation of the region of stability of the machine using the steady-state stability limit $\delta = 90°$. This turns out to be

$$P^2 + \left[Q - \frac{x_d - x_e}{2x_d x_e} E_t^2\right]^2 = \left[\frac{x_d + x_e}{2x_d x_e} E_t^2\right]^2 \qquad (1.5)$$

where $E_t = |\overline{E}_T|$ and $x_d = x_{dl}$.

The above relation represents a circle in the P-Q plane centered at $\left(0, \frac{x_d - x_e}{2x_d x_e} E_t^2\right)$, and having a radius $\left(\frac{x_d + x_e}{2x_d x_e}\right) E_t^2$. The derivation of this circle is given in Appendix A. The interior of this circle is claimed to be the stable operating region. This circle is being used for practical applications including those in the utility industry.

However, a couple of questions arise. Adams and McClure derive the circle using load flow equations alone - no machine dynamics are considered. Hence, one is tempted to ask, what is the relationship between the above stability region and the dynamic stability of the machine itself? Also, how valid is the classical machine model used?

1.2.2. Underexcitation Limiter

Underexcitation Limiters have been used since early applications of voltage regulators to generators. As mentioned previously, these limiters prevent the voltage regulators from reducing the excitation of the synchronous machine below some preset point. And the limits are set so as to prevent the machine from exceeding its steady state stability limit.

During the development stages, the field current determined by these limiters was a constant value regardless of the kW output of the machine. This prevented full utilization of the underexcited capability of generators at lighter loads, as stability limits are a function of the kW output. This was overcome in 1939 with the introduction of a limiter which responded to changes in the kW output using mechanical inputs. More exact methods became necessary with the growth of power systems, and in 1947, limiters making use of machine terminal voltage and current were installed. One of the few available descriptions of

UELs in the literature is that given by Rubenstein and Temoshok [4] back in the 50's. The limiter presented has a straight-line characteristic of the form

$$\frac{Q}{E_t^2} = K_1 - \left(\frac{P}{E_t^2}\right) K_2 \qquad (1.6)$$

In a more recent publication by Dutkiewicz and Fedora, [5] the performance of UELs during islanding is discussed. Islanding of an existing EHV network is simulated, and use of the manufacturer's suggested data to represent the limiters results in the loss of field relay tripping and island collapse due to generation deficiency. The authors are drawn to the conclusion that traditional setups for UELs may be sufficient only during slow dynamic phenomena, and that these may not allow enough time for the limiters to control the field during rapid reactive transients, which could lead to unnecessary unit tripping by the loss of field relay. Hence, margins between UELs and loss of field relays should be tailored to suit transients pertinent to their location. In addition, it is necessary to ensure that the resulting limiter curves do not encroach on the steady-state underexcited operating region.

An attempt has been made in this work to clarify some of the above issues, and to gain a better understanding of the functioning of limiters.

2. STEADY-STATE STABILITY OF A FIXED EXCITATION SYNCHRONOUS MACHINE

2.1. Introduction

This chapter investigates the steady-state stability of a synchronous machine using rigorous dynamic modeling. First, an accurate model of the system is presented, which is nonlinear, as will be seen in the next section. However, steady-state stability is concerned only with small, slow deviations occurring in the system - which permits the study of stability around an operating point. This means that the system can be linearized around an operating point, and the resulting linear system can be analyzed using any of the standard techniques available - instead of dealing with the original nonlinear system. In this work, eigenvalue analysis is used. Time-scale properties of the system model can be exploited to obtain lower order models, whose stability can also be studied in a similar manner. Finally, it is shown that a closed form expression can be derived for the region of stability in the P-Q plane.

2.2. Single Machine Model

Figure 2.1 shows the single-line diagram of the system under consideration - single machine connected to an infinite bus.

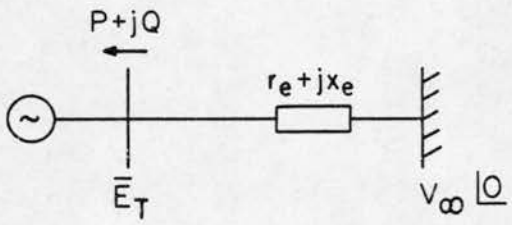

Figure 2.1. Single machine-infinite bus system.

This system can be modeled by means of six variables. The resulting equations are

$$\frac{1}{\omega_s}\frac{d\lambda_d}{dt} = -\frac{r_s + r_e}{x'_d + x_e}\lambda_d + \frac{r_s + r_e}{x'_d + x_e}E'_q + \nu\lambda_q + \sqrt{3}\,V_\infty \sin\delta \tag{2.1}$$

$$\frac{1}{\omega_s}\frac{d\lambda_q}{dt} = -\frac{r_s + r_e}{x'_q + x_e}\lambda_q - \frac{r_s + r_e}{x'_q + x_e}E'_d - \nu\lambda_d + \sqrt{3}\,V_\infty \cos\delta \tag{2.2}$$

$$T'_{do}\frac{dE'_q}{dt} = -\frac{x_d + x_e}{x'_d + x_e}E'_q + \frac{x_d - x'_d}{x'_d + x_e}\lambda_d + E_{FD} \tag{2.3}$$

$$T'_{qo}\frac{dE'_d}{dt} = -\frac{x_q + x_e}{x'_q + x_e}E'_d - \frac{x_q - x'_q}{x'_q + x_e}\lambda_q \tag{2.4}$$

$$\frac{1}{\omega_s}\frac{d\delta}{dt} = \nu - 1 \tag{2.5}$$

$$2H\frac{d\nu}{dt} = T_m + \frac{1}{3}\left[\frac{1}{x'_q + x_e} - \frac{1}{x'_d + x_e}\right]\lambda_d\lambda_q + \frac{1}{3}\frac{1}{x'_q + x_e}\lambda_d E'_d + \frac{1}{3}\frac{1}{x'_d + x_e}\lambda_q E'_q - D'\nu \tag{2.6}$$

Here, the first two equations represent stator transients - λ_d and λ_q are the d-axis and q-axis fluxes (including x_e), respectively. E'_q is a voltage proportional to the field winding flux. The machine is modeled with a damper winding on the q-axis, and its flux is represented by a proportional voltage E'_d. δ and ν are the familiar electromechanical variables. Since stability in the absence of the Automatic Voltage Regulator (AVR) is of interest, AVR and governor equations are not included. The equations are all in motor notation, and all quantities are in p.u.

2.3. Equilibrium

The next step in stability analysis is to obtain an equilibrium and linearize the model around this point. Care should be taken in choosing the external quantities to be specified for determination of equilibrium. In the model chosen for analysis, the whole system external to the machine terminals is represented by a Thevenin source $V_\infty \underline{/0}$ and an equivalent impedance Z_e. This source may be called an infinite bus in the sense that it has infinite inertia. Consider normal operating conditions when the machine is loaded with some specified P and Q. The AVR will be active, maintaining the required terminal voltage magnitude E_t. Once these quantities are fixed, the value of the Thevenin source or the infinite bus is determined by the load current. When loading conditions change, the AVR adjusts excitation to maintain E_t at the specified value. For a new load current, the voltage magnitude at the infinite bus will be different. In other words, the Thevenin source is operating-point dependent.

During perturbations around an operating point, however, the infinite bus maintains constant voltage owing to its inertia. If the AVR is lost, the terminal voltage magnitude cannot be controlled any further - the machine excitation remains constant. So during a transient when the AVR is lost, the external system is represented by an infinite bus, while the machine itself has constant excitation.

The system model (Equations (2.1) to (2.6)) is of the form

$$\frac{dX}{dt} = f(X,U) \tag{2.7}$$

where X is the set of state variables and U is the set of inputs (T_m and E_{FD}). An equilibrium is obtained by setting the right-hand side of the above equation to zero, i.e.,

$$f(X,U) = 0$$

and solving the resulting algebraic equations simultaneously. From synchronous machine theory, the following steady-state relations can be obtained.

$$\lambda_d = E_q' + (x_d' + x_e)\, i_d \tag{2.8}$$

$$\lambda_q = x_q i_q = -E_d' + (x_q' + x_e)\, i_q \tag{2.9}$$

$$V_d = \sqrt{3}\, V_\infty \sin \delta \tag{2.10}$$

$$V_q = \sqrt{3}\, V_\infty \cos \delta \tag{2.11}$$

where V_d and V_q are the d- and q-axis components of V_∞, and i_d and i_q are the d- and q-axis components of the load current. From (2.5), at equilibrium, $\nu = 1.0$ p.u. From (2.1) and (2.2) using (2.8)-(2.11),

$$-(r_s + r_e)\, i_d + (x_q + x_e)\, i_q + V_d = 0 \tag{2.12}$$

$$-(r_s + r_e)\, i_q + (x_d + x_e)\, i_d - x_{md}\, i_{fd} + V_q = 0 \tag{2.13}$$

where i_{fd} is the field current. These equations can be reduced to the form

$$\overline{V}_\infty = Z\overline{I}_a + \overline{E}_a \tag{2.14}$$

where

$$Z = (r_s + r_e) + j(x_q + x_e) \tag{2.15}$$

$$E_a = \left[(x_d - x_q)\, I_a \sin(\delta - \theta_i) + \frac{x_{md}\, i_{fd}}{\sqrt{3}}\right] e^{j\delta} \tag{2.16}$$

and $\overline{I}_a = I_a \angle\theta_i$ is the load current. Hence, the machine can be represented by a source (with phase angle δ) in series with an impedance $r_s + jx_q$. Now the equilibrium values can be calculated as follows.

Given the complex power $\overline{S} = P + jQ$ and the terminal voltage magnitude E_t

$$\text{Compute } \overline{I}_a = \frac{P - jQ}{E_t \angle 0^\circ} \tag{2.17}$$

Hence

$$\overline{V}_\infty = V_\infty \angle\alpha = E_t \angle 0^\circ + (r_e + jx_e)\, \overline{I}_a \tag{2.18}$$

Since the infinite bus has been used as a reference in the model equations, the actual phasors will be,

$$\overline{E}_T = E_t \angle -\alpha \tag{2.19}$$

$$\overline{I}_a = I_a \angle \theta_i - \alpha \tag{2.20}$$

$$\overline{E}_a = \overline{E}_T - (r_s + jx_q)\, \overline{I}_a \tag{2.21}$$

$$\delta = \text{angle of } \overline{E}_a \tag{2.22}$$

The field current i_{fd} can be calculated from (2.16) as

$$|\overline{E}_a| = (x_d - x_q)\, I_a \sin(\delta - \theta_i) + \frac{x_{md}\, i_{fd}}{\sqrt{3}} \tag{2.23}$$

Using the relation

$$i_d + ji_q = \sqrt{3}\, \overline{I}_a\, e^{j(\pi/2 - \delta)} \tag{2.24}$$

one can obtain i_d and i_q from which the remaining variables can be evaluated.

$$\lambda_d = (x_d + x_e)\, i_d + x_{md}\, i_{fd} \tag{2.25}$$

$$\lambda_q = (x_q + x_e)\, i_q \tag{2.26}$$

$$E'_q = \lambda_d - (x'_d + x_e)\, i_d \tag{2.27}$$

$$E'_d = (x'_q + x_e)\, i_q - \lambda_q \tag{2.28}$$

The above values are used to evaluate the A and B matrices in the linearized form of Equations (2.1) to (2.6),

$$\dot{\Delta X} = A\Delta X + B\Delta U \tag{2.29}$$

and the eigenvalues of A are calculated. This can be done for any desired value of P, Q and E_t, and a region of stability can be traced out in the P-Q plane by observing the signs of eigenvalues at different points.

2.4. An Example

As an example, consider a turbogenerator with the following parameters:

$x_d = x_q = 1.79 \quad x'_d = 0.355 \quad x'_q = 0.57 \quad D' = 0$

$r_s = 0 \quad T'_{do} = 7.9 \quad T'_{qo} = 0.41$

The external system has negligible resistance, and has an equivalent system reactance $x_e = 0.215$. The problem is to determine the machine's region of stability in the P-Q plane when $E_t = 1.0$ p.u.

For P = 1.0, Q = 0.35, Equations (2.17) to (2.22) yield the following equilibrium conditions:

$V_\infty = 1.09653 \quad \delta = -89.52° \quad \overline{E}_T = 1.0 \angle -11.31°$

These, along with values obtained from Equations (2.25) to (2.28), are used

to evaluate the A-matrix of Equation (2.29). Under the above conditions, it yields the eigenvalues shown in Table 2.1.

The ±j377.0 eigenvalues correspond to stator transients (λ_d, λ_q). The other complex pair arises due to electromechanical variables δ and ω. The real eigenvalue -0.0025 is due to E'_q, and the remaining one due to E'_d. The given conditions form a stable operating point, since all eigenvalues have negative real parts. Keeping P fixed, the value of Q can be varied until one eigenvalue goes to zero. This is found to occur for two values of Q - once in the overexcited region, and once in the underexcited region. Both cases are shown in Table 2.1.

TABLE 2.1.

SYSTEM EIGENVALUES FOR SIXTH ORDER MODEL

Q = 0.35	Q = 0.36	Q = -4.46
0.0 ± j377	0.0 ± j377	0.0 ± j377
-0.42 ± j8.71	-0.42 ± j8.70	-0.44 ± j2.11
-0.0025	+0.0002	+0.0351
-6.229	-6.229	-6.229

Note that in both cases it is the E'_q eigenvalue that goes unstable. Repeating the procedure for various values of P and Q yields the region of stability shown in Figure 2.2.

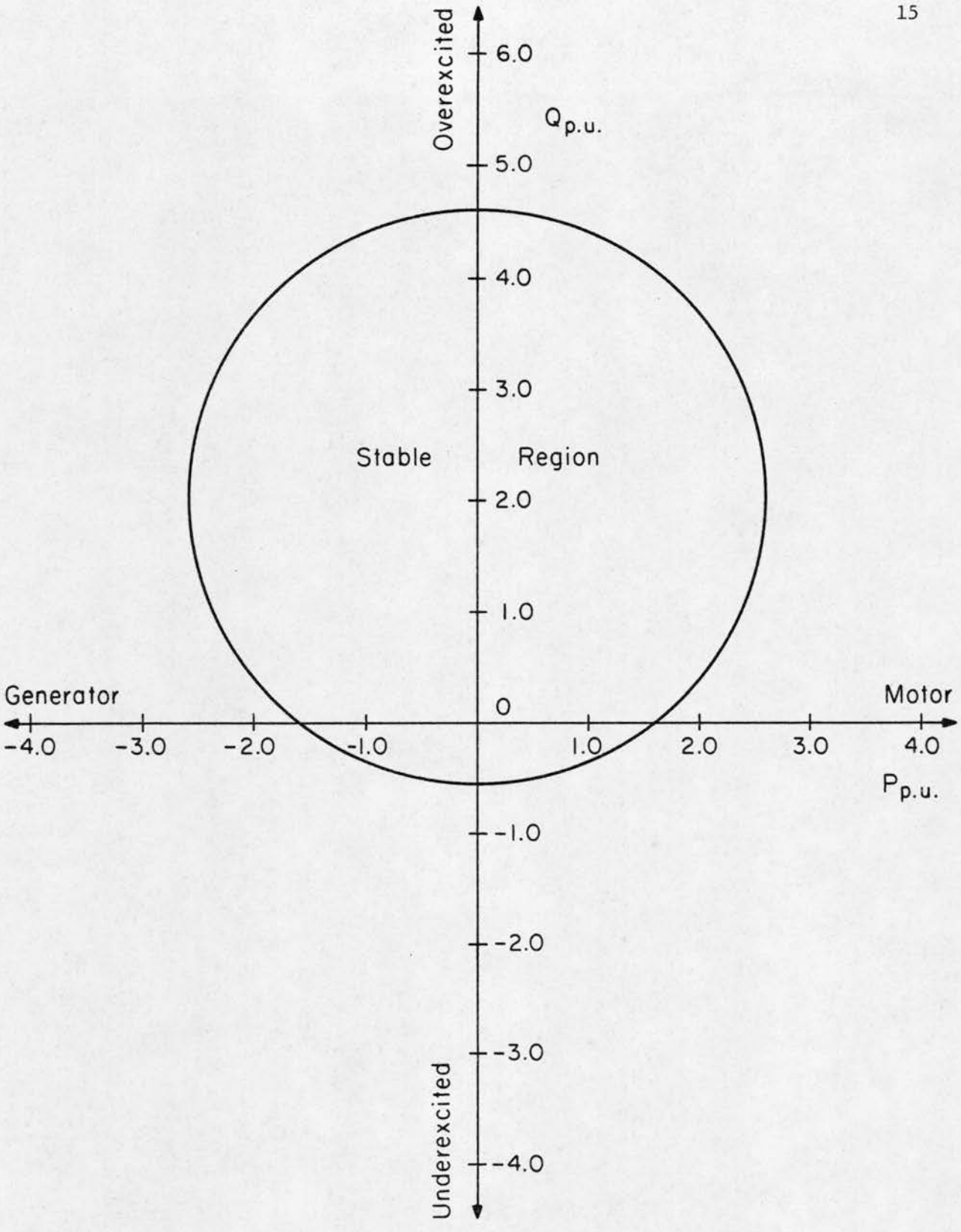

Figure 2.2. Stability region of a fixed excitation synchronous machine.

2.5. Fourth Order Model

As mentioned earlier, time-scale properties can be used to obtain reduced order models of the system under consideration. But for the case when $r_s = r_e = 0$ Equations (2.1) and (2.2) can be solved independent of the rest - and have the solution, $\lambda_d = \sqrt{3}\, V_\infty \cos \delta$, $\lambda_q = -\sqrt{3}\, V_\infty \sin \delta$. Substitution of the above into Equations (2.3) to (2.6) results in a fourth order model, commonly known as the two-axis model. Its state equations are

$$T'_{do} \frac{dE'_q}{dt} = - \frac{x_d + x_e}{x'_d + x_e} E'_q + \frac{x_d - x'_d}{x'_d + x_e} \sqrt{3}\, V_\infty \cos \delta + E_{FD} \tag{2.30}$$

$$T'_{qo} \frac{dE'_d}{dt} = - \frac{x_q + x_e}{x'_q + x_e} E_d + \frac{x_q - x'_q}{x'_q + x_e} \sqrt{3}\, V_\infty \sin \delta \tag{2.31}$$

$$\frac{1}{\omega_s} \frac{d\delta}{dt} = \nu - 1 \tag{2.32}$$

$$2H \frac{d\nu}{dt} = T_m - \frac{1}{2} \left[\frac{1}{x'_q + x_e} - \frac{1}{x'_d + x_e} \right] V_\infty^2 \sin 2\delta$$

$$+ \frac{1}{\sqrt{3}} \frac{1}{x'_q + x_e} V_\infty E'_d \cos \delta - \frac{1}{\sqrt{3}} \frac{1}{x'_d + x_e} V_\infty E'_q \sin \delta - D'\nu \tag{2.33}$$

The stability region can be evaluated here also by the same procedure as for the sixth order model. Again, the eigenvalues for $E_t = 1.0$, $P = 1.0$ are shown in Table 2.2 for various Q.

TABLE 2.2.

SYSTEM EIGENVALUES FOR FOURTH ORDER MODEL

Q = 0.35	Q = 0.36	Q = -4.46
-0.42 ± j8.71	-0.42 ± j8.70	-0.44 ± j2.11
-0.0025	+0.0002	+0.0351
-6.229	-6.229	-6.229

Comparing this with the sixth order case given in Table 2.1 reveals that four of the eigenvalues are identical, confirming the statement that the stator transients form an isolated subsystem. Also, instability occurs at the same values of P & Q, and the E'_q eigenvalue is once again the culprit. The region of stability is the same as the one shown in Figure 2.2.

2.6. Third and Second Order Models

Using singular perturbation, further order reduction can be obtained - in fact, the third order flux decay model can be derived by eliminating E'_d as a fast variable. The resulting equations (as T'_{qo} goes to zero) are

$$T'_{do} \frac{dE'_q}{dt} = - \frac{x_d + x_e}{x'_d + x_e} E'_q + \frac{x_d - x'_d}{x'_d + x_e} \sqrt{3}\, V_\infty \cos \delta + E_{FD} \tag{2.34}$$

$$\frac{1}{\omega_s} \frac{d\delta}{dt} = \nu - 1 \tag{2.35}$$

$$2H \frac{d\nu}{dt} = T_m - \frac{1}{2}\left[\frac{1}{x_q + x_e} - \frac{1}{x'_d + x_e}\right] V_\infty^2 \sin 2\delta$$

$$- \frac{1}{\sqrt{3}} \frac{1}{x'_d + x_e} V_\infty E'_q \sin \delta - D'\nu \qquad (2.36)$$

This model also yields the same stability region as the sixth and fourth order models, with the E'_q eigenvalue being the cause of instability once again.

A second order model can be derived from the above by considering a slow field winding, and again using perturbation theory. The resulting constant $E'_q (=E'^{o}_q)$ model has the dynamic equations,

$$\frac{1}{\omega_s} \frac{d\delta}{dt} = \nu - 1 \qquad (2.37)$$

$$2H \frac{d\nu}{dt} = T_m - \frac{1}{2}\left[\frac{1}{x_q + x_e} - \frac{1}{x'_d + x_e}\right] V_\infty^2 \sin 2\delta$$

$$- \frac{1}{\sqrt{3}} \frac{1}{x'_d + x_e} E'^{o}_q V_\infty \sin \delta - D'\nu$$

and yields a stability region different from the previous ones (Figure 2.3). Note that the region produced by electromechanical modes alone is much larger.

Yet another second order model can be derived by considering the damper winding also to be slow. This is the constant E'_q, constant E'_d model with the dynamic equations

$$\frac{1}{\omega_s} \frac{d\delta}{dt} = \nu - 1$$

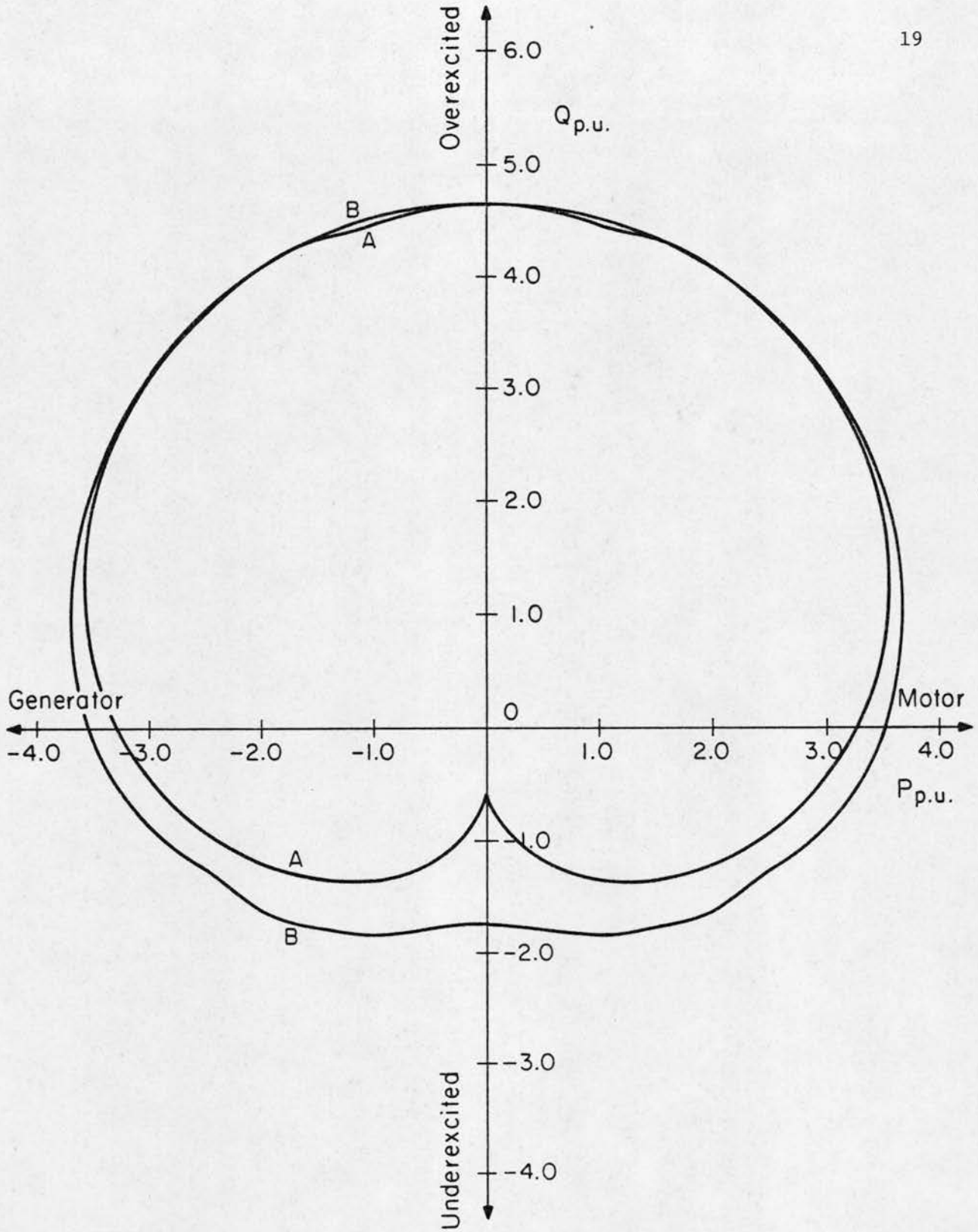

Figure 2.3. Stability regions of the second order models. A. Constant E'_q. B. Constant E'_q, Constant E'_d.

$$2H \frac{d\nu}{dt} = T_m - \frac{1}{2}\left[\frac{1}{x'_q + x_e} - \frac{1}{x'_d + x_e}\right] V_\infty^2 \sin 2\delta$$

$$- \frac{1}{\sqrt{3}} \frac{1}{x'_d + x_e} V_\infty E'^{o}_q \sin \delta + \frac{1}{\sqrt{3}} \frac{1}{x'_q + x_e} V_\infty E'^{o}_d \cos \delta - D'\nu \quad (2.40)$$

Its stability region is also shown in Figure 2.3. Once again, the region is much larger and does not coincide with any of the previous cases.

2.7. Analytical Derivation

From the discussion so far one can conclude that the stability region of a fixed excitation synchronous machine is determined by its field winding eigenvalue. In this section, an analytical expression for this region is obtained from the dynamic equations by considering the field winding flux to be the slowest variable with all others fast variables.

Rewriting Equation (2.34),

$$T'_{do} \frac{dE'_q}{dt} = - \frac{x_d + x_e}{x'_d + x_e} E'_q + \frac{x_d - x'_d}{x'_d + x_e} \sqrt{3}\, V_\infty \cos \delta + E_{FD}$$

Or

$$T'_d \frac{dE'_q}{dt} = -E'_q + \frac{x_d - x'_d}{x_d + x_e} \sqrt{3}\, V_\infty \cos \delta + \frac{x'_d + x_e}{x_d + x_e} E_{FD} \quad (2.41)$$

Linearizing about the point P_o, Q^o, V_∞^o, δ^o, E'^{o}_q, T_m^o

$$T'_d \frac{d}{dt} \Delta E'_q = -\Delta E'_q - \frac{x_d - x'_d}{x_d + x_e} \sqrt{3}\, V_\infty^o \sin \delta^o \, \Delta\delta \quad (2.42)$$

Considering δ and ν as fast variables, the quasi-steady-state equation is

$$T_m - \frac{1}{2}\left[\frac{1}{x_q + x_e} - \frac{1}{x'_d + x_e}\right] V_\infty^{o2} \sin 2\delta^o - \frac{1}{\sqrt{3}} \frac{1}{x'_d + x_e} V_\infty^o E_q'^o \sin \delta^o = 0 \quad (2.43)$$

Taking differentials around the operating point,

$$0 - \frac{1}{2}\left[\frac{1}{x_q + x_e} - \frac{1}{x'_d + x_e}\right] V_\infty^{o2} \cdot 2 \cos 2\delta^o \cdot \Delta\delta - \frac{1}{\sqrt{3}} \frac{1}{x'_d + x_e} V_\infty^o E_q'^o \cos \delta^o \Delta\delta$$

$$- \frac{1}{\sqrt{3}} \frac{1}{x'_d + x_e} V_\infty^o \sin \delta^o \Delta E_q = 0 \quad (2.44)$$

which gives

$$\Delta\delta = - \frac{V_\infty^o \sin \delta^o / \sqrt{3} \, (x'_d + x_e)}{\frac{V_\infty^o E_q'^o \cos \delta^o}{\sqrt{3}(x'_d + x_e)} + \left[\frac{1}{x_q + x_e} - \frac{1}{x'_d + x_e}\right] V_\infty^{o2} \cos 2\delta^o} \Delta E'_q \quad (2.45)$$

Substituting into the single slow Equation (2.42),

$$T'_d \frac{d}{dt} \Delta E'_q = \left[\frac{\frac{x_d - x'_d}{x_d + x_e} \sqrt{3} V_\infty \sin \delta^o \cdot \frac{V_\infty^o \sin \delta^o}{\sqrt{3}(x'_d + x_e)}}{\frac{V_\infty^o E_q'^o \cos \delta^o}{\sqrt{3}(x'_d + x_e)} + \frac{(x'_d - x_q) V_\infty^{o2} \cos 2\delta^o}{(x_q + x_e)(x'_d + x_e)}} - 1 \right] \Delta E_q \quad (2.46)$$

Rearranging terms, the stability condition becomes

$$\frac{V_\infty^o E_q'^o \cos \delta^o}{\sqrt{3}(x_d' + x_e)} + \frac{V_\infty^{o2} \cos 2\delta^o}{(x_q + x_e)} + \left[\frac{1}{x_d + x_e} + \frac{1}{x_d' + x_e}\right] V_\infty^{o2} \sin^2 \delta^o \geq \frac{V_\infty^{o2}}{x_d' + x_e} \tag{2.47}$$

with the equality indicating the boundary of the stability region. Hence, for a round rotor machine, at the boundary,

$$\frac{V_\infty^o E_q'^o \cos \delta^o}{\sqrt{3}(x_d' + x_e)} + \frac{V_\infty^{o2} \cos 2\delta^o}{(x_d + x_e)} + \left[\frac{1}{x_d + x_e} + \frac{1}{x_d' + x_e}\right] V_\infty^{o2} \sin^2 \delta^o - \frac{V_\infty^{o2}}{x_d' + x_e} = 0 \tag{2.48}$$

Or

$$\frac{V_\infty^o E_q'^o \cos \delta^o}{\sqrt{3}(x_d' + x_e)} - \frac{V_\infty^{o2} \sin^2 \delta^o}{(x_d + x_e)} - \frac{V_\infty^{o2} \cos^2 \delta^o}{(x_d' + x_e)} + \frac{V_\infty^{o2}}{x_d + x_e} = 0 \tag{2.49}$$

If Q_∞^o is the reactive power input at the infinite bus, then by definition,

$$Q_\infty^o = \lambda_d^o i_d^o + \lambda_q^o i_q^o \tag{2.50}$$

Using proper substitutions, it can be shown that

$$Q_\infty = \frac{V_\infty^{o2} \sin^2 \delta^o}{(x_d + x_e)} + \frac{V_\infty^{o2} \cos^2 \delta^o}{(x_d' + x_e)} - \frac{V_\infty^o E_q'^o \cos \delta^o}{\sqrt{3}(x_d' + x_e)} \tag{2.51}$$

Hence, Equation (2.49) simplifies to

$$-Q_\infty^o + \frac{V_\infty^{o2}}{(x_d + x_e)} = 0 \tag{2.52}$$

Now

$$Q_\infty^o = Q^o + I_a^2 x_e \tag{2.53}$$

where Q^o is the operating point reactive power. Also,

$$\overline{I}_a^o = \left[P^o - jQ^o\right] / \overline{E}_T^{o*}$$

$$I_a^{o2} = (P^{o2} + Q^{o2}) / E_t^{o2} \tag{2.54}$$

$$Q_\infty^o = Q^o + \frac{(P^{o2} + Q^{o2})\, x_e}{E_t^{o2}} \tag{2.55}$$

Combining (2.52) and (2.55),

$$P^{o2} + Q^{o2} + \frac{E_t^{o2}}{x_e} Q^o = \frac{E_t^{o2}}{x_e} \cdot \frac{V_\infty^{o2}}{(x_d + x_e)} \tag{2.56}$$

The stability regions derived in the previous sections all have a fixed E_t for the entire region - while V_∞^o varies depending on loading conditions, as mentioned earlier. Hence an equation for the region can be obtained if V_∞^o is eliminated from the above equation.

Let $\overline{E}_T^o = E_t^o \angle \theta^o$

$$\overline{V}_\infty^o = V_\infty^o \angle 0 = E_t^o \angle \theta^o + jx_e \frac{P^o - jQ^o}{E_t^o \angle -\theta^o} \tag{2.57}$$

Or

$$V_\infty^o E_t^o \angle -\theta^o = E_t^{o2} + x_e(Q^o + jP^o) \tag{2.58}$$

$$V_\infty^{o2} E_t^{o2} = (E_t^{o2} + x_e Q^o)^2 + (x_e P^o)^2 \tag{2.59}$$

Or

$$\frac{V_\infty^{o2} E_t^{o2}}{x_e(x_d + x_e)} = \frac{E_t^{o4}}{x_e(x_d + x_e)} + \frac{x_e}{x_d + x_e}(P^{o2} + Q^{o2}) + \frac{2Q^o E_t^{o2}}{(x_d + x_e)} \tag{2.60}$$

Combining (2.56) and (2.60),

$$P^{o2} + Q^{o2} + \frac{E_t^{o2}}{x_e} Q^o = \frac{x_e}{x_d + x_e}(P^{o2} + Q^{o2}) + \frac{2E_t^{o2}}{(x_d + x_e)} Q^o + \frac{E_t^{o4}}{x_e(x_d + x_e)}$$

Rearranging,

$$\frac{x_d}{x_d + x_e} P^{o2} + \frac{x_d}{x_d + x_e} Q^{o2} + \left[\frac{1}{x_e} - \frac{2}{x_d + x_e}\right] E_t^{o2} Q^o = \frac{E_t^{o4}}{x_e(x_d + x_e)} \tag{2.62}$$

Or

$$P^{o2} + Q^{o2} + \frac{x_d - x_e}{x_d x_e} E_t^{o2} Q^o = \frac{E_t^{o4}}{x_d x_e} \tag{2.63}$$

Completing squares for the Q^o terms,

$$P^{o2} + \left[Q^o + \frac{x_d - x_e}{2x_d x_e} E_t^{o2}\right]^2 = E_t^{o4}\left[\frac{1}{x_d x_e} + \frac{(x_d - x_e)^2}{4x_d^2 x_e^2}\right]$$

Or,

$$P^{o2} + \left[Q^o + \frac{x_d - x_e}{2x_d x_e} E_t^{o2}\right]^2 = \left[\frac{x_d + x_e}{2x_d x_e} E_t^{o2}\right]^2 \tag{2.64}$$

Since E_t^o is a constant, the above equation represents a circle in the P-Q plane, with center $(0, -\frac{x_d - x_e}{2x_d x_e} E_t^{o2})$ and radius $\frac{x_d + x_e}{2x_d x_e} E_t^{o2}$. It may be easily verified that this circle coincides with the stability regions of sixth, fourth

and third order models. It is also interesting to note that the above circle can be derived from purely algebraic conditions, with the stipulation that $\delta = 90°$ at the stability boundary.

The above analysis did not use $\delta = 90°$ as a criterion for stability. Alternatively, it used an analytical approximation for the eigenvalue associated with the mode which was reponsible for the stability region boundary. There are two interesting points here. First the approximation of the slowest eigenvalue (field flux mode) appears to give an exact characterization of the smallest stability region. Secondly, this region is also characterized by $\delta = 90°$ which is normally thought of as a condition for instability in the electromechanical modes.

3. STEADY-STATE STABILITY OF A REGULATED SYNCHRONOUS MACHINE

3.1. Introduction

The region of stability derived in Chapter 2 has only limited applications, as it is true only for a machine stripped of all its controls. Each of the numerous control subsystems that are essential in a modern machine have associated dynamics, and each additional state variable brings about modifications in the stability region. In the sections that follow, two such controls are presented. First, an excitation system - IEEE Type 1 - and its effect on machine stability is discussed, then the control of particular interest in this work, the Underexcitation Limiter with special emphasis on its model and the significance of various parameters with regard to steady state stability.

3.2. Excitation Control

The excitation system utilized in this work falls into the IEEE Type 1 category [7]. The model shown in Figure 3.1 comprises a continuously acting regulator and exciter. Continuous regulation implies that the control signal is always present, and initiates corrective action proportional to the system error. Thus, it is sensitive to even minor changes in the controlled variable, namely the terminal voltage magnitude (E_t).

The first time constant T_r, which represents first order smoothing or filtering of the regulator input is not significant in most systems, and hence may be considered zero. The first summing junction determines the error in the input signal, and this is combined with the stabilizing signal at the subsequent junction. The regulator amplifier transfer function is represented as a gain K_A and a time constant T_A. Limits are imposed on the amplifier output to prevent large error signals from causing outputs which exceed practical limits of components. In the next stage, the exciter is represented by a transfer

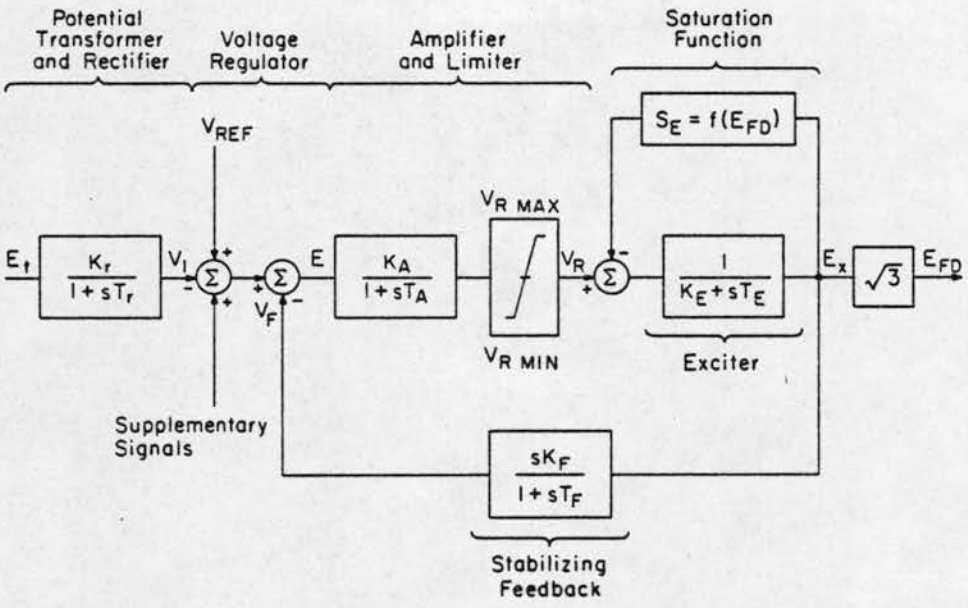

Figure 3.1. IEEE Type 1 excitation system.

function $1/(K_E + S_E)$ and a saturation function $S_E = f(E_{FD})$. A scaling factor $\sqrt{3}$ has been introduced so that an exciter output of 1 p.u. results in 1 p.u. terminal voltage. The derivative feedback V_F provides the necessary damping in the system. The system dynamic model is given by

$$E_{FD} = \sqrt{3}\, E_X \tag{3.1}$$

$$T_E \frac{dE_x}{dt} = V_R - (K_E + S_E)\, E_X \tag{3.2}$$

$$T_A \frac{dV_R}{dt} = -V_R + K_A(V_{REF} - V_F - E_t) \tag{3.3}$$

$$T_F \frac{dV_F}{dt} = -V_F + \frac{K_F}{T_E}(V_R - (K_E + S_E)\, E_X) \tag{3.4}$$

Thus the dynamics of three additional variables come into play in deciding the stability of a regulated machine. To study the changes, the third order

machine model (Equations (2.34) to (2.36)) was combined with the above equations, and the resulting sixth order model was subjected to eigenvalue analysis. The linearized stability matrix used is given in Appendix B. The machine and system constants used can be found in Section 2.4, and the excitation system constants are shown in Table 3.1.

TABLE 3.1.

EXCITATION SYSTEM CONSTANTS

Constant	Value	Constant	Value
K_r	1.0	K_E	-0.05
T_r	0.0	S_E	0.
K_A	20.0	T_E	0.314
T_A	0.2	$V_{R\ MAX}$	2.1
K_F	0.063	$V_{R\ MIN}$	-1.0
T_F	0.35		

The region of stability for E_t = 1.0 is plotted in Figure 3.2 along with the stability circle derived in the absence of the regulator.

Once again, the region is symmetric about the Q-axis. The only improvement of any consequence is that in the underexcited mode. Though the region has contracted slightly for low values of P, there is significant gain at higher values - about 0.25 p.u. of Q at P = 1.0 p.u., for example. This wider margin can be beneficially employed in various situations. It must be borne in mind that the size and shape of the region depends on E_t, the chosen terminal voltage and other constants associated with the particular regulator.

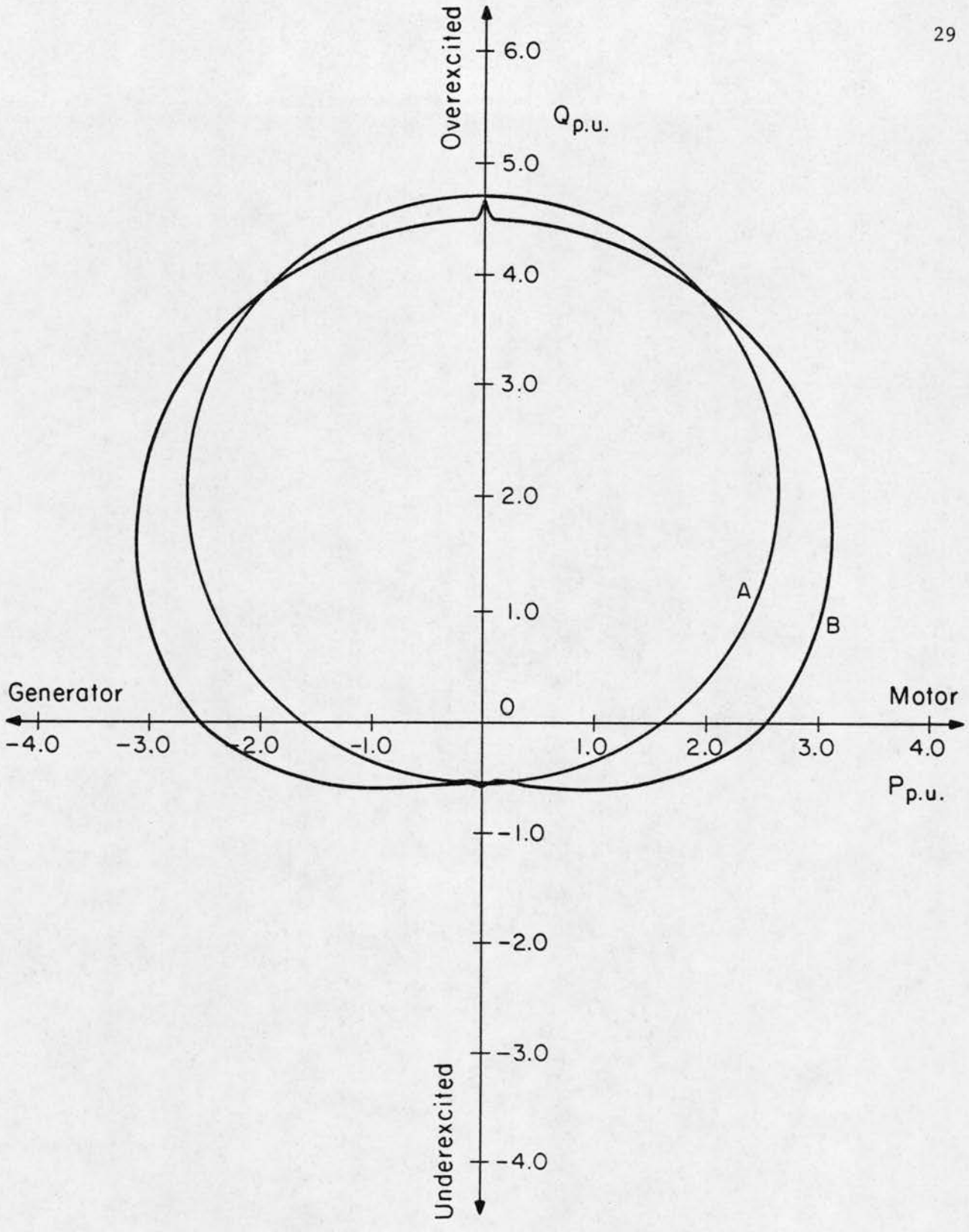

Figure 3.2. Steady-state stability limit of a synchronous machine. A. Without AVR. B. With AVR.

3.3. The Underexcitation Limiter (UEL)

The purpose of the UEL is to limit machine excitation to some prespecified minimum value. The specification of this minimum being in terms of reactive power, (or a characteristic in the P-Q plane) the device should be able to respond to Q directly. Some additional considerations in designing such a device would be (a) a response that is fast enough to stabilize the machine during a contingency (b) minimum inherent dynamics (c) the use of simple available inputs and (d) a flexible output characteristic with simple controls.

A model which accounts for the effects of the limiter on the generator and its subsystems is shown in Figure 3.3 [5]. $\bar{E}_T$ and $\bar{I}_T$ are the generator terminal voltage and load current respectively (both in p.u.). V_F is the damping feedback voltage to the automatic voltage regulator, which is zero for steady-state operation. The constants K_R, K_C and K_I are referred to as Radius control,

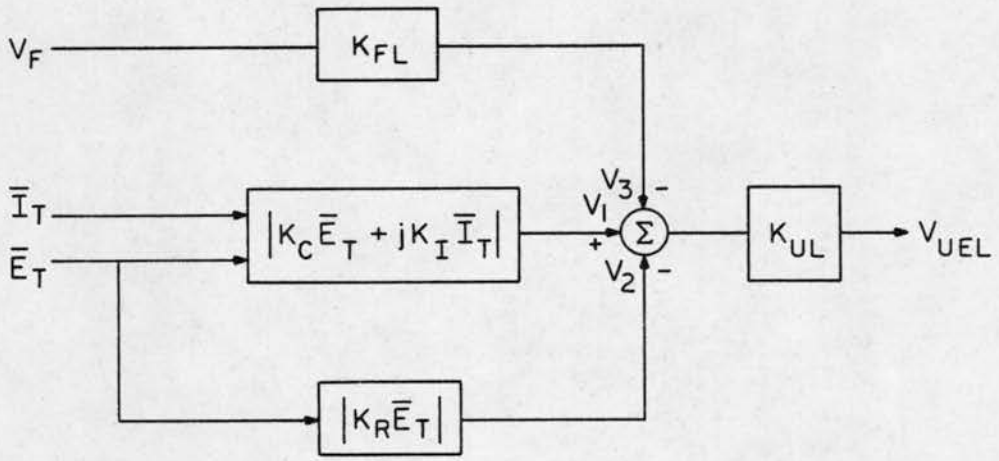

Figure 3.3. Underexcitation Limiter model.

Center control and Current control respectively, and their values depend on the steady-state stability characteristic of the particular machine. (The voltage

V_I must be such that it increases as the reactive power absorbed by the machine increases. Hence, appropriate sign change should be made depending on notation - generator or motor - of equations used in simulations. All quantities are in motor notation here.)

As an example, consider the sample machine of Chapter 2, which has a stability region of radius 2.6 p.u. centered on the reactive axis at 2.05 p.u. Typical values of the control constants could be $K_R = 2.6$, $K_C = 2.05$ and $K_I = 0.55$ (intercept of SSSL on the reactive axis). Typical values for the gains K_{FL} (damping feedback gain) and K_{UL} (limiter gain) are [5]

$$1.0 \leq K_{FL} \leq 4.0$$

$K_{UL} = K_A/4$ (K_A - regulator amplifier gain)

The characteristic generated by these constants can be obtained in the following manner.

Assume some P and Q into the machine at some specified terminal voltage E_t. Using Equations (2.17) through (2.20), $\overline{E}_T$ and $\overline{I}_T$ can be evaluated. These are substituted into the model in Figure 3.3 to find V_{UEL} ($V_F = 0$ in steady state). Keeping P fixed, Q is varied until V_{UEL} becomes zero. The procedure is repeated for various P's so as to cover the required region in the P-Q plane. Table 3.2 shows the results obtained for $E_t = 0.95$ p.u., $x_e = 0.215$ p.u., $K_R = 2.6$, $K_C = 2.05$ and $K_I = 0.55$. Note that the reactive part of $\overline{I}_T$ is around 1 p.u. As mentioned previously, the limiter characteristic can be altered by changing the constants in the model. Table 3.3 shows the effect of variations in K_I, the current control.

TABLE 3.2.

LIMITER CURVE FOR $K_R = 2.6$, $K_C = 2.05$, $K_I = 0.55$ AND $E_t = 0.95$

P	Q	$\overline{I}_T$
0.0	0.91	0.0 - j0.96
-0.1	0.91	-0.09 - j0.96
-0.2	0.90	-0.17 - j0.95
-0.3	0.90	-0.26 - j0.96
-0.4	0.89	-0.35 - j0.97
-0.5	0.88	-0.43 - j0.97
-0.6	0.87	-0.52 - j0.98
-0.7	0.85	-0.61 - j0.99
-0.8	0.83	-0.69 - j1.00
-0.9	0.81	-0.78 - j1.01
-1.0	0.79	-0.87 - j1.02
-1.1	0.76	-0.96 - j1.03
-1.2	0.74	-1.04 - j1.06

TABLE 3.3.

VARIATION OF LIMITER CHARACTERISTIC WITH K_I

ALL OTHER QUANTITIES AS IN TABLE 3.2.

P	Q_1	Q_2	Q_3
	$K_I = 0.35$	$K_I = 0.55$	$K_I = 0.75$
0.0	1.42	0.91	0.67
-0.1	1.42	0.91	0.67
-0.2	1.42	0.90	0.66
-0.3	1.42	0.90	0.65
-0.4	1.41	0.89	0.64
-0.5	1.40	0.88	0.63
-0.6	1.40	0.87	0.61
-0.7	1.39	0.85	0.59
-0.8	1.38	0.83	0.56
-0.9	1.36	0.81	0.53
-1.0	1.35	0.79	0.50

The effect is very clear - the region of operation in the underexcited mode is restricted as K_I increases. But increasing K_R, the radius control, has just the opposite consequence - as can be seen in Table 3.4.

TABLE 3.4.

VARIATION OF LIMITER CHARACTERISTIC WITH K_R

ALL OTHER QUANTITIES AS IN TABLE 3.2.

P	Q_1	Q_2	Q_3
	$K_R = 2.4$	$K_R = 2.6$	$K_R = 2.8$
0.0	0.58	0.91	1.24
-0.1	0.58	0.91	1.23
-0.2	0.57	0.90	1.23
-0.3	0.56	0.90	1.23
-0.4	0.55	0.89	1.22
-0.5	0.53	0.88	1.21
-0.6	0.52	0.87	1.20
-0.7	0.50	0.85	1.18
-0.8	0.48	0.83	1.17
-0.9	0.45	0.81	1.15
-1.0	0.42	0.79	1.13

Another significant factor with regard to limiter characteristics is the terminal voltage. The dependence is illustrated in Table 3.5. This dependence becomes relevant during reactive transients, etc. - when too high or too low a terminal voltage may result in the limiter characteristic being wide off the mark.

A proper choice of K_R, K_C and K_I can thus be utilized to set the limiter characteristic as desired. The setting itself should take into account a number of other factors such as a loss of field relay setting, required operating region in the underexcited mode, etc.

TABLE 3.5.

VARIATION OF LIMITER CHARACTERISTIC WITH E_t

ALL OTHER QUANTITES AS IN TABLE 3.2.

P	Q_1	Q_2
	$E_t = 0.95$	$E_t = 1.0$
0.0	0.91	1.0
-0.1	0.91	1.0
-0.2	0.90	1.0
-0.3	0.90	1.0
-0.4	0.89	0.99
-0.5	0.88	0.98
-0.6	0.87	0.97
-0.7	0.85	0.95
-0.8	0.83	0.94
-0.9	0.81	0.92
-1.0	0.79	0.90

Finally, what is the effect of the UEL on system steady-state stability? To answer this question, it is necessary to decide how to coordinate the UEL signal with the rest of the system. UEL action is necessary when Q goes beyond the set characteristic. And the action should be in the form of excitation control, since terminal voltage (and hence Q) is directly dependent on excitation. As excitation control during normal operation is done by the voltage regulator, it is logical to conclude that the UEL signal should be given priority over the regulator signal during contingencies of interest. The steady-state analysis of the UEL reveals that its output behaves like an error signal with respect to Q, (or equivalently E_t) being negative in the safe zone, zero on the characteristic, and positive beyond. So the required excitation control can be achieved by substituting the UEL output for the regulator error signal during emergencies.

So the dynamic equations representing the excitation system with the UEL signal given preference to the regulator error signal read

$$E_{FD} = \sqrt{3}\, E_x \tag{3.5}$$

$$T_E \frac{dE_x}{dt} = V_R - (K_E + S_E)\, E_x \tag{3.6}$$

$$T_A \frac{dV_R}{dt} = -V_R + K_A\, V_{UEL} \tag{3.7}$$

$$T_F \frac{dV_F}{dt} = -V_F + \frac{K_F}{T_E} (V_R - (K_E + S_E)\, E_x) \tag{3.8}$$

where V_{UEL} is the UEL output.

System stability can now be analyzed by combining the above equations with the machine equations - (2.34) to (2.36). The linearized sixth order stability matrix can be found in Appendix B.

The limiter gain K_{UL} becomes a crucial factor in deciding system stability in the steady state. To illustrate this, consider the equilibrium P = -1.0, Q = 0.382, E_t = 1.0285 (refer to Section 4.2.5 for further details). The results of eigenvalue analysis of this equilibrium for different values of K_{UL} are shown in Table 3.6.

At K_{UL} = 0.18, the system becomes just unstable. Reducing limiter gain below this critical value in a practical setting results in an unstable operating point. So unusually low settings for K_{UL} should be avoided, since it can be a definite source of instability.

The limiter model presented here does not involve any dynamics. This may not be valid always. For example, the actual implementation may involve delays. This can be accounted for by the addition of a time constant in the given model.

TABLE 3.6.

SYSTEM EIGENVALUES FOR DIFFERENT LIMITER GAINS

$K_R = 2.4$, $K_I = 0.7$, $K_C = 2.05$

OTHER CONSTANTS AS IN TABLE 3.1

K_{UL}	5.0	1.0	0.5	0.15
Eigen-	-3.84 ± j23.91	-3.8 ± j10.72	-3.73 ± j7.46	-3.84 ± j3.89
values	-0.97 ± j8.93	-0.165 ± j8.81	-0.277 ± j8.84	-0.24 ± j8.97
	-9.139 ± j0.899	-0.104 ± j0.871	-0.069 ± j0.835	0.0144 ± j0.693

4. SYSTEM PERFORMANCE AND UNDEREXCITATION LIMITERS

4.1. Introduction

The importance of UEL performance during reactive transients was briefly touched upon in Chapter 1. In this chapter, an attempt is made to give this idea a sound basis via an illustration. The system performance during a relevant contingency is studied, with and without UEL. It is shown that the system becomes unstable in the absence of UEL, and that the AVR alone is insufficient to limit instability in the underexcited mode, although it improves the region of safe operation. It is also shown that the stabilizing action of the UEL depends on a judicious choice of the quantities involved.

4.2. Illustration

4.2.1. The disturbance

Parallel operation of generators in a power system involves sharing of the net reactive power demand. Consider two generators operating in parallel in the underexcited mode. If one of the units is lost, the other would be driven further into the underexcited region - even beyond its SSSL. This is a real-life situation which calls for UEL action.

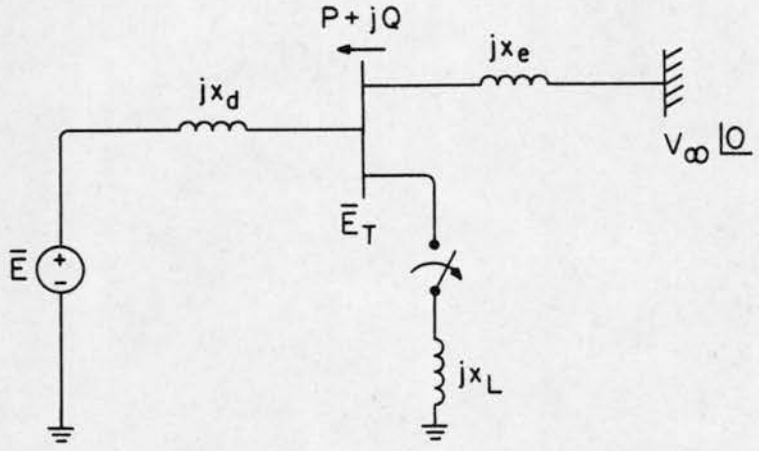

Figure 4.1. The fault simulated.

The scenario is similar to the one shown in Figure 4.1 (p. 37). Here, the machine is loaded by an inductor at its terminals in addition to the external system represented by the infinite bus and the reactance jx_e. At some instant $t = t_{sw}$, the inductive load is thrown off. A reactive transient ensues, during which the external system, owing to its high inertia, continues demanding the same real and reactive power. As a consequence, the machine will be pushed further into the underexcitation region (assuming AVR is functioning properly) - the final steady state being determined by the magnitude of jx_L. This disturbance is analyzed in detail in the following sections.

4.2.2. Non-linear simulation model

In developing an elementary state-space model for analysis of the system in Figure 4.1, it is necessary to account for (a) the machine (b) the external system, including x_L (c) the voltage regulator and (d) the UEL. The various other control systems involved are of little interest in the present case.

In Figure 4.1, the entire system external to the machine terminals (including x_L) can be Thevenized to give a voltage source $V'_\infty \angle 0$ in series with a reactance jx'_e. Thus, the system prior to switching can be reduced to the single machine-infinite bus system dealt with in Chapter 2. After switching, the system structure remains identical, only the values of the Thevenin equivalent change. Thus, any of the models presented in Chapter 2 can be used for simulation - the one axis (flux decay) model is used here. (Equations (2.34) to (2.36)).

To include the effects of the UEL on the system response, the IEEE Type 1 excitation subsystem presented in Chapter 3 was modified as shown in Figure 4.2. The only addition is a simple two input High Value (HV) gate. If A and B are its inputs and C the output,

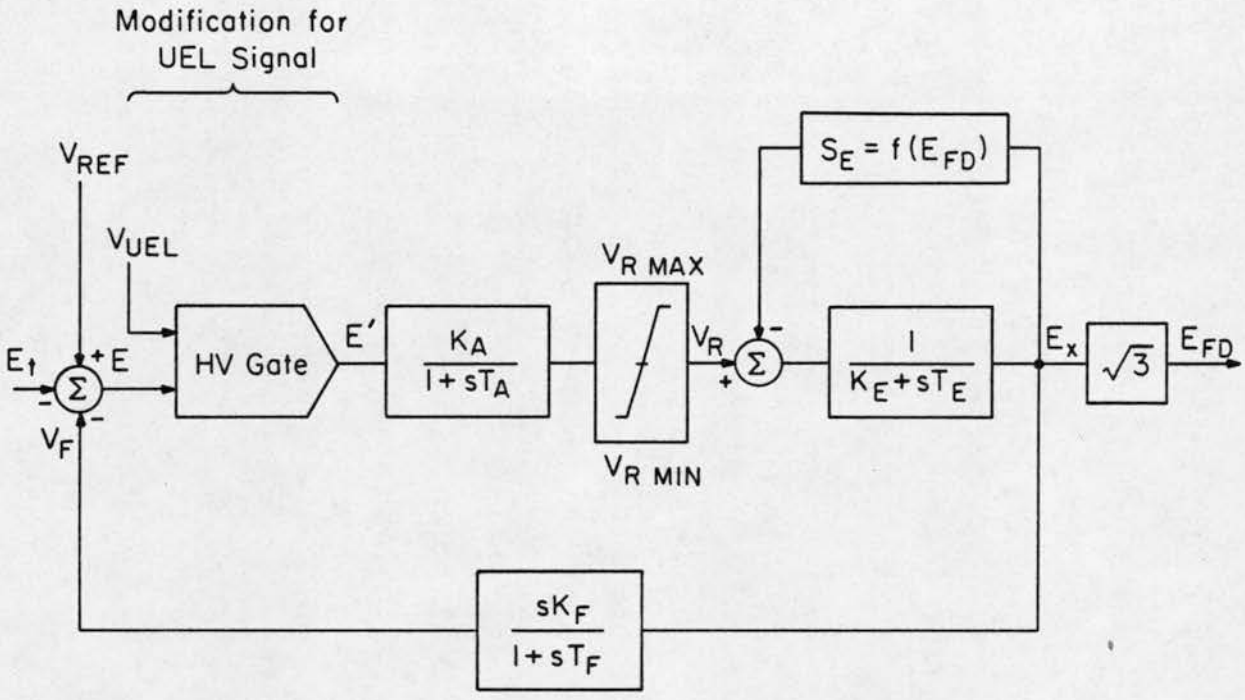

Figure 4.2. Modified regulator-exciter subsystem.

$C = A \quad \text{if} \quad A > B$

$C = B \quad \text{if} \quad B > A$

Here, the choice is between E, the regulator error signal and V_{UEL}, the output of the underexcitation limiter. Hence as soon as the UEL signal becomes larger than E, it takes control of the exciter. The resulting state equations are

$$E_{FD} = \sqrt{3}\, E_x \tag{4.1}$$

$$T_E \frac{dE_x}{dt} = V_R - (K_E + S_E)\, E_x \tag{4.2}$$

$$T_A \frac{dV_R}{dt} = -V_R + K_A\, E' \tag{4.3}$$

$$E' = \text{Max}(V_{UEL}, E) \tag{4.4}$$

$$V_{UEL} = K_{UL}[\,|K_C\bar{E}_T + jK_I\bar{I}_T| - |K_R\bar{E}_T| - K_{FL}V_F] \tag{4.5}$$

$$E = V_{REF} - E_t - V_F \tag{4.6}$$

$$T_F \frac{dV_F}{dt} = -V_F + \frac{K_F}{T_E} (V_R - (K_E + S_E) E_x) \tag{4.7}$$

Equation (4.5) is obtained from the UEL model given in Figure 3.1.

The machine and system constants used for simulation are given in Section 2.4. The excitation system constants were as shown in Table 3.1. The UEL characteristic was chosen so as to coincide with the SSSL of the machine. This required $K_R = 2.4$, $K_c = 2.05$ and $K_I = 0.70$. K_{UL} was chosen to be $5.0 (= K_A/4)$, and K_{FL} was 2.0.

The initial conditions were $E_t = 1.0$ p.u., $P = -1.0$ p.u. (generator) and $Q = -0.1$ p.u. (overexcited). x_L was chosen to be 1.67 p.u. such that the final equilibrium ($E_t = 1.0$ p.u., $P = -1.0$ p.u., $Q = 0.5$ p.u.) was outside the SSSL of the unregulated machine, but within the stable operating region in the presence of the AVR. The load x_L was thrown off at $t = 0.5$ sec, and the system response was obtained by numerical integration of the state space model.

4.2.3. Case 1: System response without the UEL

First, the system response without the UEL signal was studied. For this, Equation (4.4) was modified as

$$E' = E \tag{4.8}$$

The results are shown in Figure 4.3. In spite of the fact that the final equilibrium is within the safe operating region, the system becomes unstable around $t = 4.5$ sec. At the switching instant, the terminal voltage jumps up by about 10%, since a reactive load is being thrown off. This causes the AVR to take corrective action by reducing E_x (and hence E'_q). But in

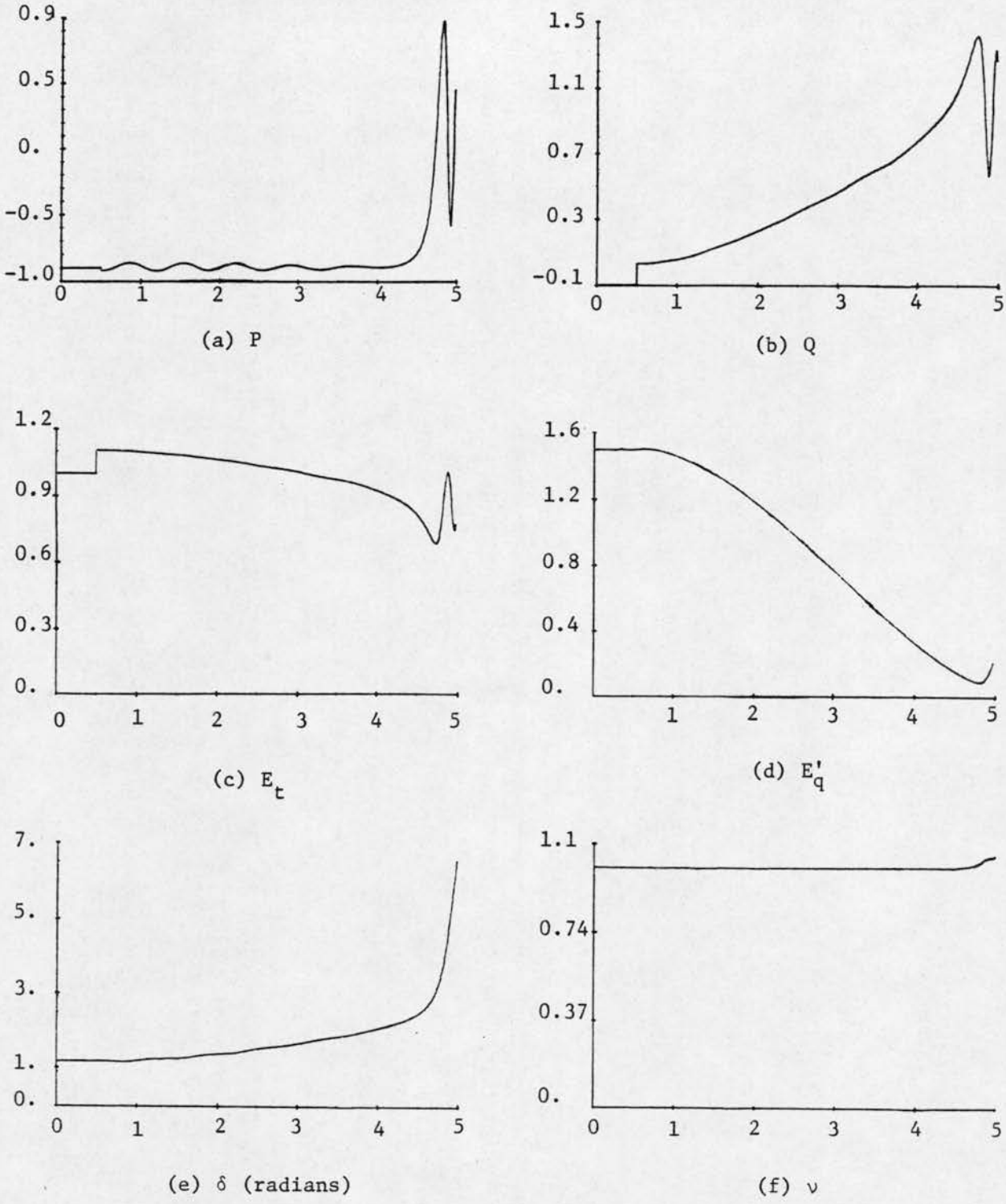

Fig. 4.3 System response without UEL. All quantities (p.u.) plotted vs. time (sec.).

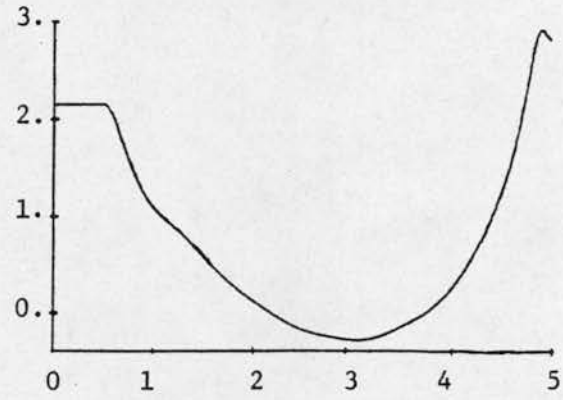

(g) E_x

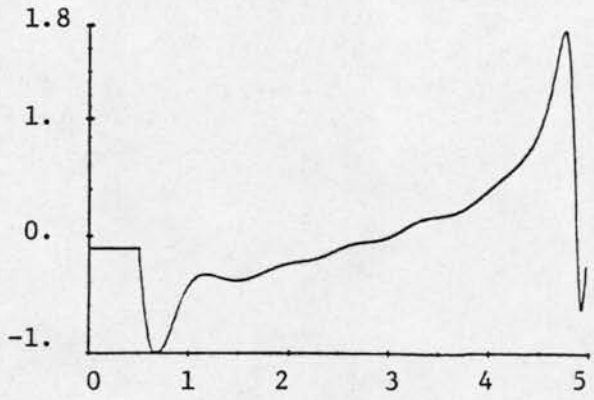

(h) V_R

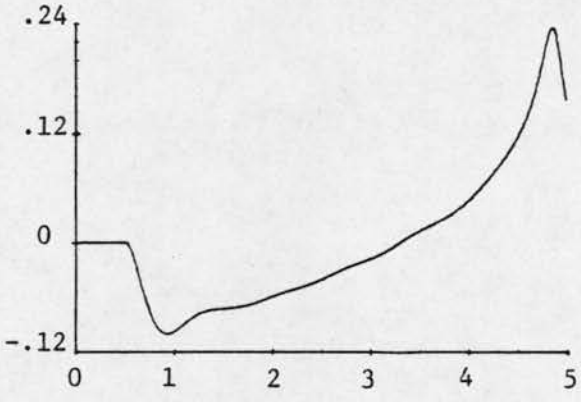

(i) V_F

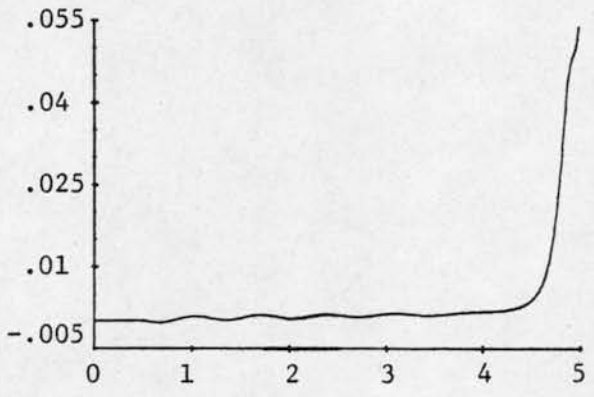

(j) ν_{rel}

Fig. 4.3(cont.) System response without UEL. All quantities (p.u.) plotted vs. time (sec.).

the process, the field flux magnitude gets reduced drastically, which results in instability. It is also to be noted that the value of Q went much beyond the safe operating region.

An interesting analogy may be drawn here to a real power transient stability disturbance. The power-angle curve of a system operating at P_1 is shown

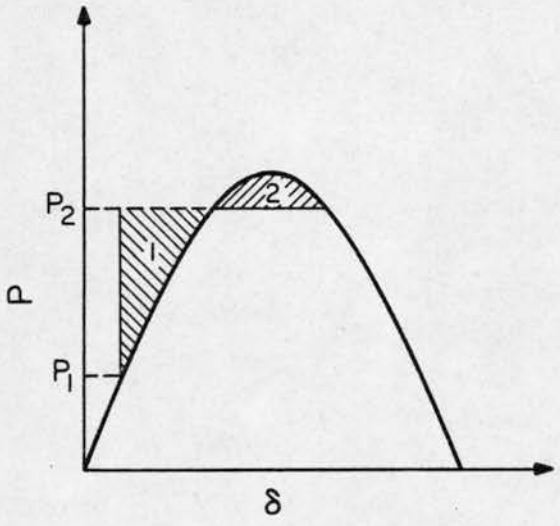

Figure 4.4. Power-angle curve.

in Figure 4.4. Both P_1 and P_2 represent stable equilibrium points - but the transition from P_1 to P_2 becomes impossible when Area 1 is larger than Area 2. Here, both the initial and final equilibrium points chosen were stable. But the transition from Q = -0.1 to Q = +0.5 could not be achieved and the system became unstable.

4.2.4. Case 2: UEL performance without damping

In deriving the steady-state UEL characteristics in Section 3.3, the damping signal V_F was set to zero (as is true in steady-state). So it is of importance to consider how well those characteristics hold good in the absence of V_F - in other words, it is worthwhile to ask, is the damping signal

redundant? This is verified in this section, by dynamic simulation of the system with the UEL, but with $K_{FL} = 0.0$.

Figure 4.5 presents the results. There is definite improvement over the previous case where the UEL is inactive. The limiter is acting as desired - as is clear from the plot of Q vs. t. The UEL output (Figure 4.5(k)) does follow Q, becoming positive when its limit is reached. Figure 4.5(l) shows a plot of $E_l (= V_{UEL} - E)$ vs. t from which the periods of UEL domination of the exciter can be determined. The UEL output becomes dominant at its set limit, but the delays caused by T_A, T_E and T'_{do} result in further lowering of Q before it is reversed. This should be taken into account while deciding upon UEL settings.

As Figures 4.5 (g,h) show, the periods of UEL override have an unwelcome consequence - the regulator output hits its upper limit, which is translated into high peaks in the exciter output. This forces the terminal voltage to go high. As soon as Q is within the safe region, the UEL loses control and the high terminal voltage stirs the AVR into corrective action, which forces events back to square one - low terminal voltage, heavy underexcitation, UEL override. The plots show the growing amplitude of the signals even after 20 seconds.

To get out of this situation, it is clear that some modification is necessary in UEL performance. The root of the problem was that the amplifier output was peaking during periods of UEL domination. This can be overcome by regulating the amplifier input - i.e., the UEL output. A simple reduction in gain would be insufficient, since it would only result in the system being more sluggish, which is not desirable. A signal which responds quickly to changes in the amplifier output would be the best choice to regulate the UEL performance. A study of the plots shows that the damping feedback V_F has adequate qualifications.

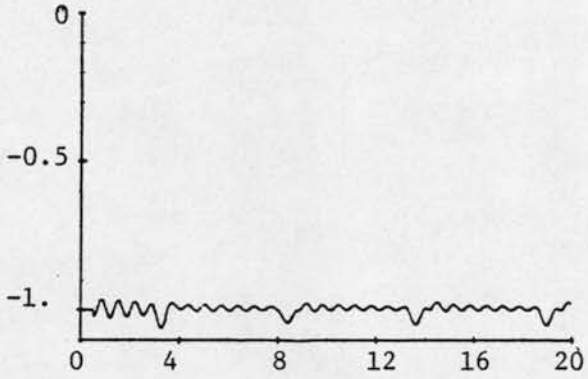

(a) P

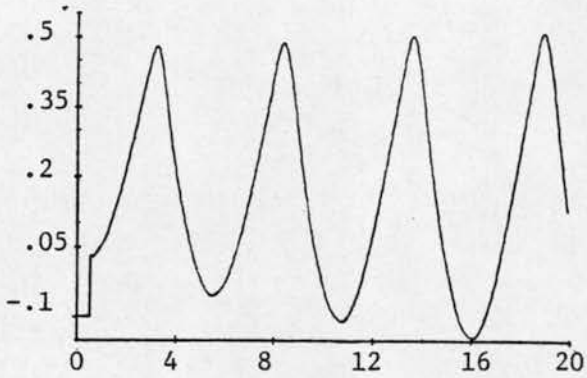

(b) Q

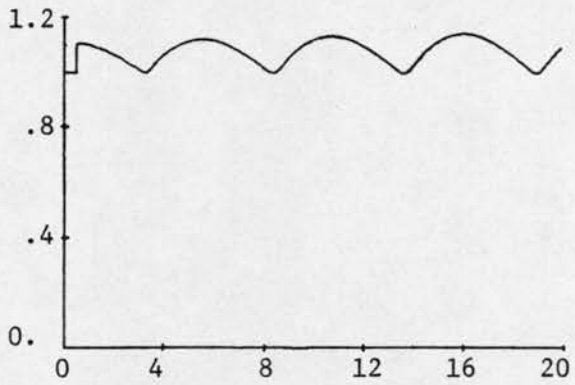

(c) E_t

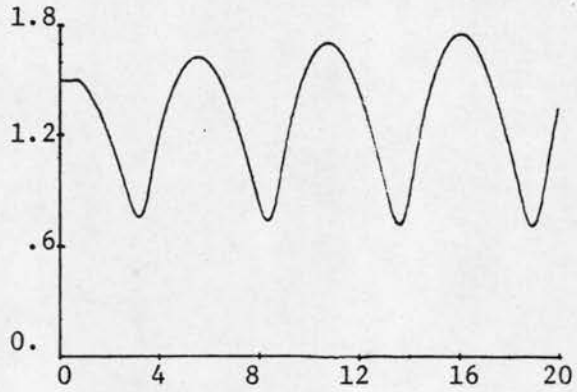

(d) E'_q

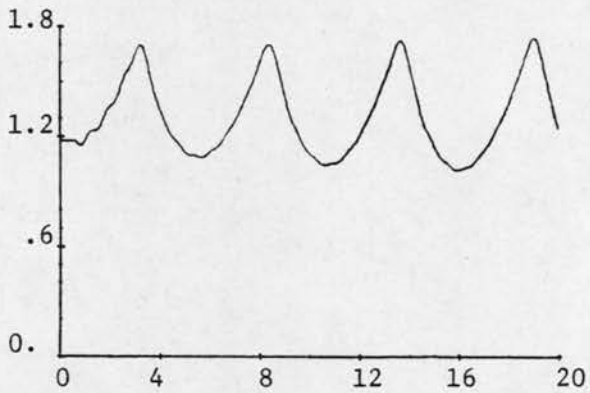

(e) δ (radians)

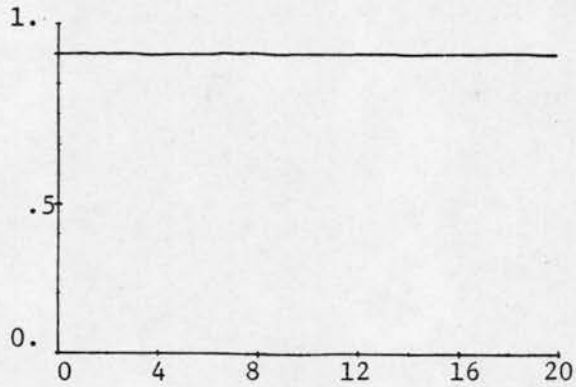

(f) ν

Fig. 4.5 System response with UEL, but no damping. All quantities (p.u.) plotted against time (sec.).

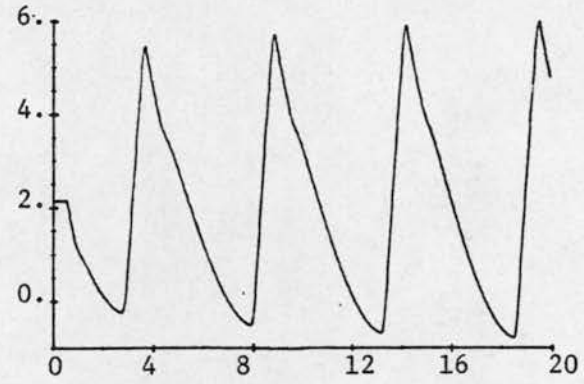

(g) E_x

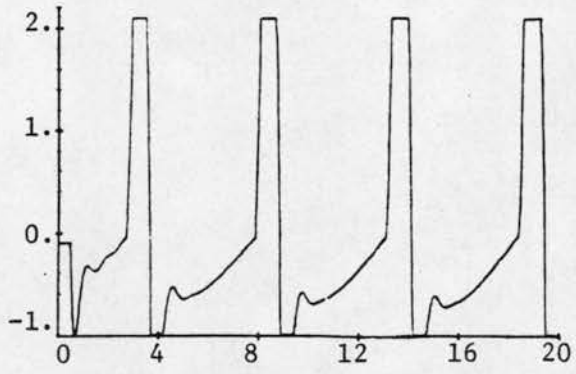

(h) V_R

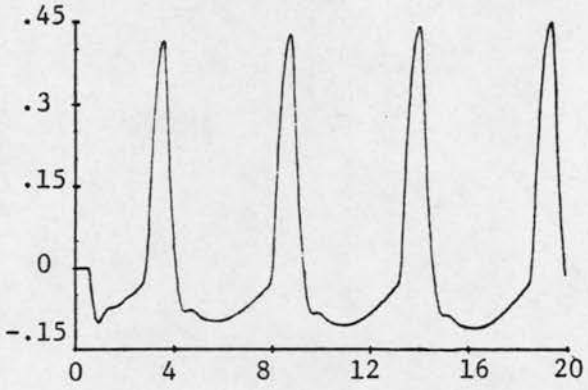

(i) V_F

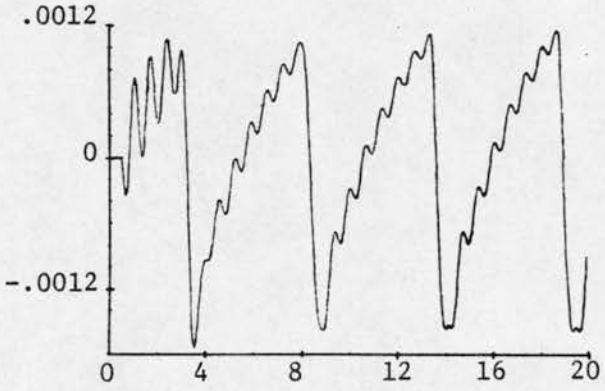

(j) ν_{rel}

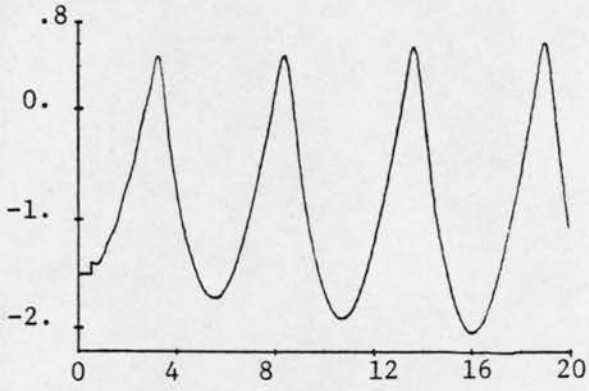

(k) V_{UEL}

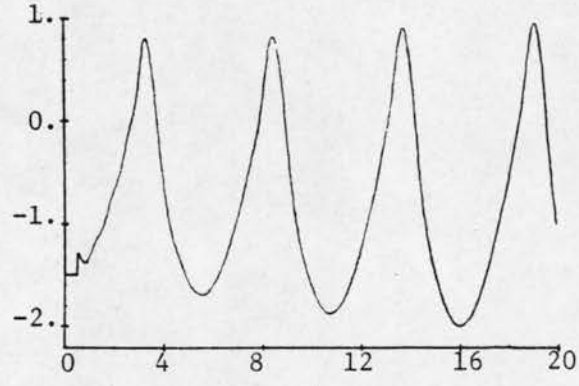

(l) $(V_{UEL}-E)$

Fig. 4.5(cont.) System response with UEL, but no damping. All quantities (p.u.) plotted against time (sec.).

4.2.5. Case 3: UEL performance with damping

Results of the dynamic simulation for the case with damping on UEL are shown in Figure 4.6. The presence of V_F results in a stable system response.

It is interesting to observe the changes in further detail. First, the sharp peaks in the UEL output do not exist anymore - the same goes for V_R, E_x, etc. As expected, the order of magnitude of V_{UEL} has been reduced. And the initial duration of domination is much longer compared to the previous case. Although lengthier, the reduced order of the UEL output ensures a stable transition.

The final equilibrium also deserves mention. The chosen point, E_t = 1.0 p.u., P = -1.0 p.u., Q = 0.5 p.u. is beyond the set characteristic of the UEL - i.e., it requires an excitation level lower than that allowed by the UEL setting. Hence, the final equilibrium will be at the same real power level, but at a higher terminal voltage (the excitation being held up by the UEL) and a correspondingly lower Q. In the simulated case, the values are found to be P = -1.0 p.u., Q = 0.382 p.u., and E_t = 1.0285 p.u.

The cost of this improvement in system performance is reflected in the plot of Q vs. t. Without damping, Q was restricted to around 0.48 p.u. (Figure 4.5(b)). But now, with the damping signal, Q goes up to about 0.58 in its first swing. Hence, in actual settings, K_{FL} should be adjusted to an optimum value based on worst case simulations.

4.2.6. Case 4: UEL performance with reduced gain

The steady-state stability of a single-machine-infinite bus system with the UEL active was considered in Chapter 3. It was found that reduction in K_{UL} leads to loss of steady-state stability, as dictated by eigenvalues. A study of transient performance under similar conditions should also lead to similar conclusions. This section attempts to verify the fact.

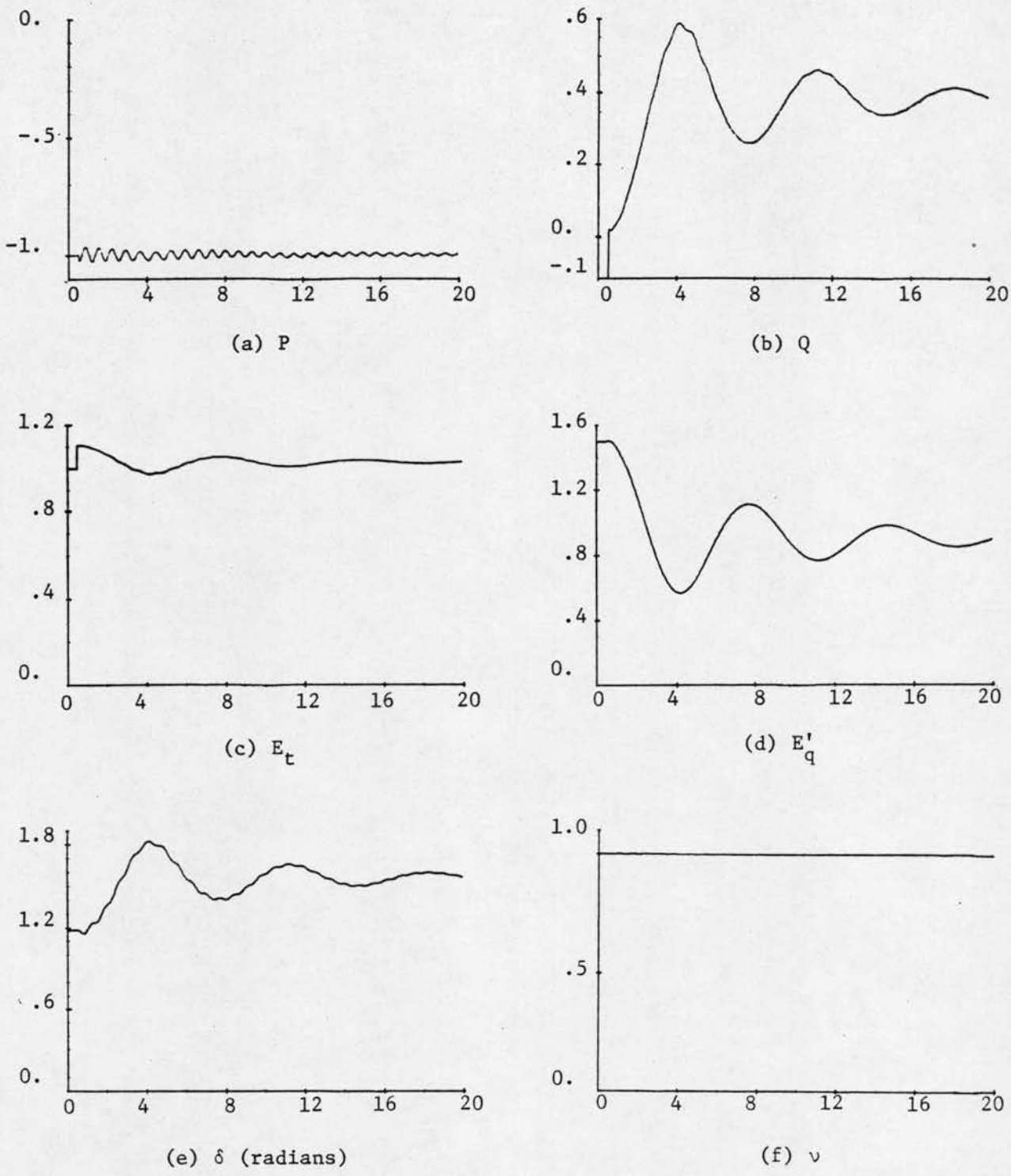

Fig. 4.6 System response with damping on UEL. All quantities (p.u.) plotted against time (sec.).

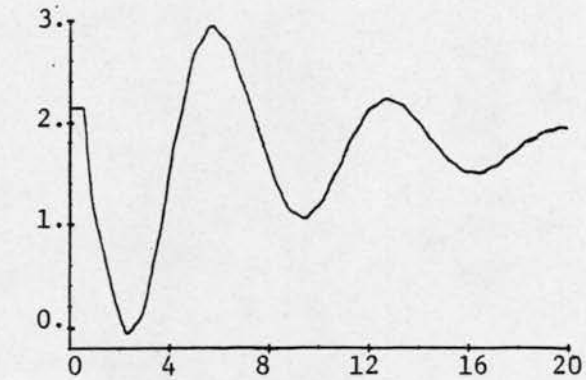

(g) E_x

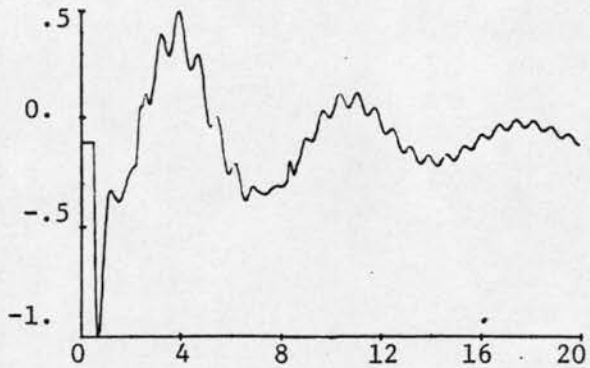

(h) V_R

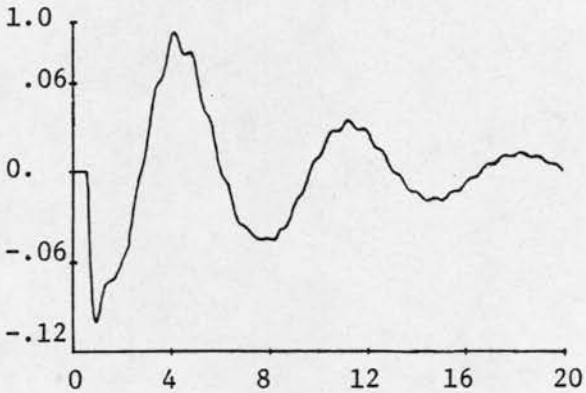

(i) V_F

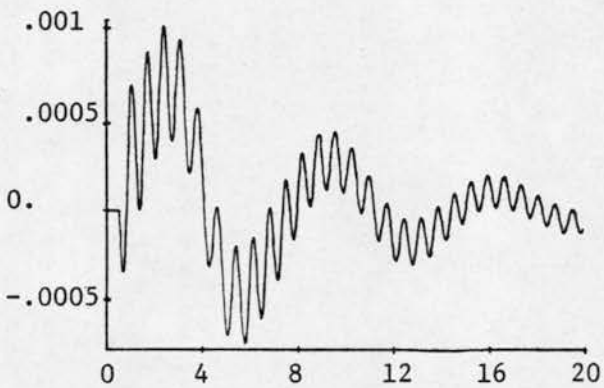

(j) ν_{rel}

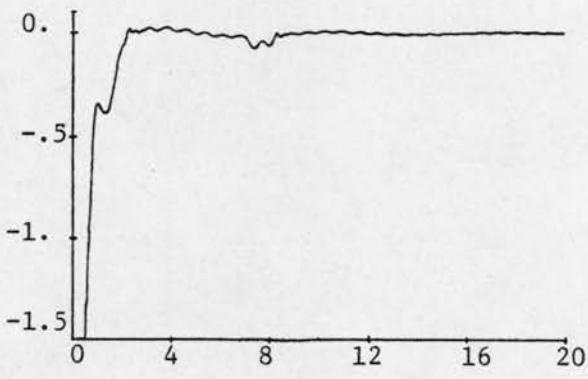

(k) V_{UEL}

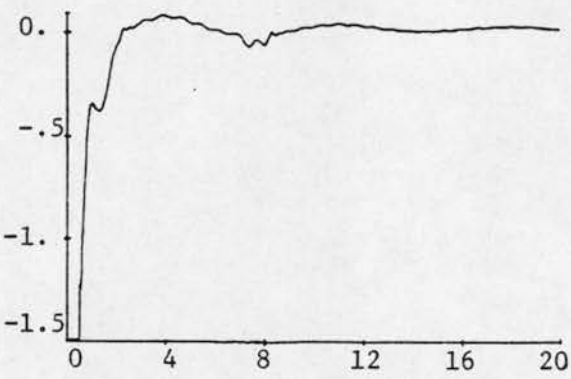

(l) $(V_{UEL}-E)$

Fig. 4.6(cont.) System response with damping on UEL. All quantities (p.u.) plotted against time (sec.).

Results of simulation for the case $K_{UL} = 0.1$ are shown in Figure 4.7. The system becomes unstable - as predicted by eigenvalue analysis. Here, the UEL is in control of the excitation from the instant of switching. But the low value of the gain makes its response ineffective. Thus, though it checks Q on the first upward swing, it is unable to provide sufficient damping during the downward swing. Because of the low gain, it retains control even after V_{UEL} becomes negative. The excitation as a result becomes very low, and the system goes unstable.

It is hoped that the discussions in this chapter give a feel for the operation of a limiter during contingencies. Of course, each emergency involving UELs is bound to have its own peculiarities, but the purpose of this treatise has been to highlight the important general features by the choice of a situation representative of a host of others.

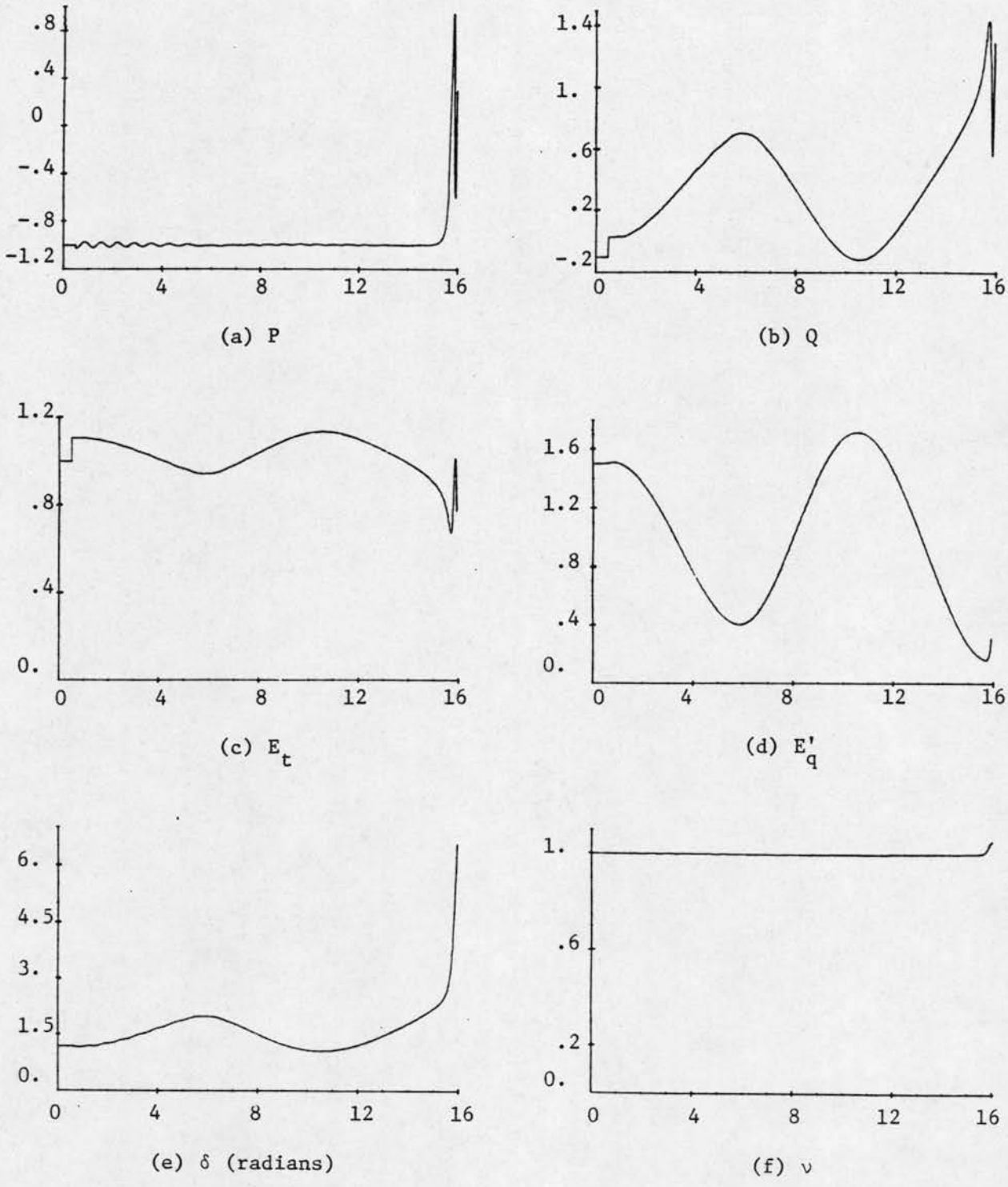

Fig. 4.7 System response with reduced UEL gain. All quantities (p.u.) plotted against time (sec.).

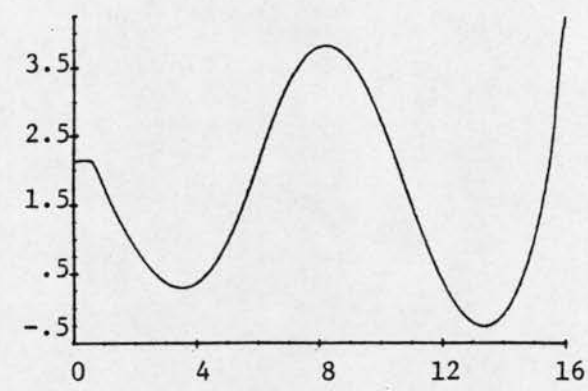

(g) E_x

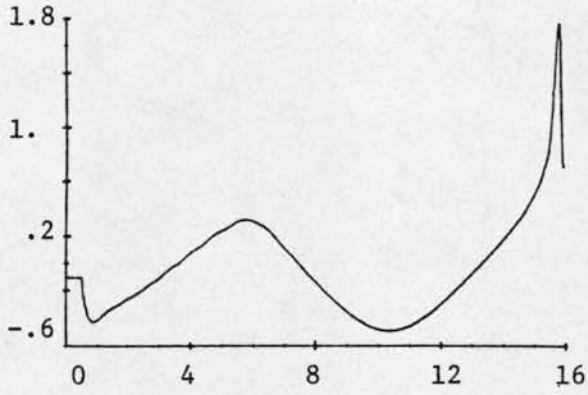

(h) V_R

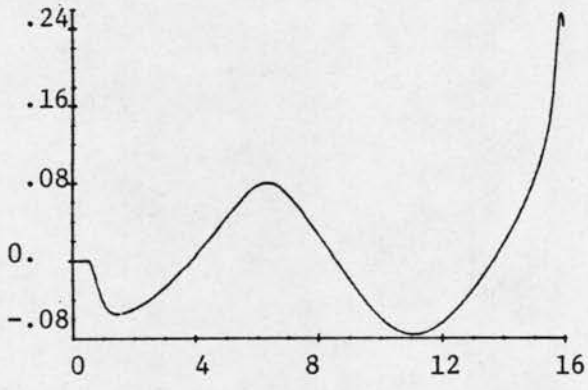

(i) V_F

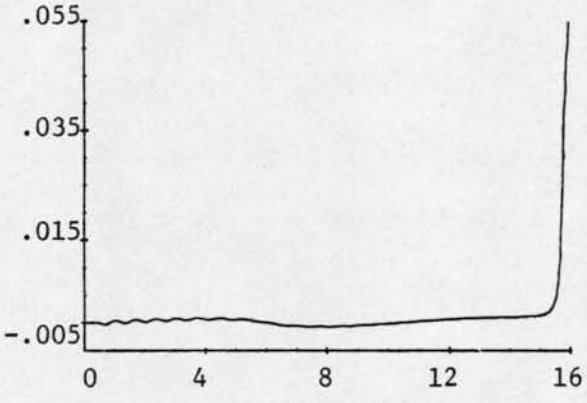

(j) ν_{rel}

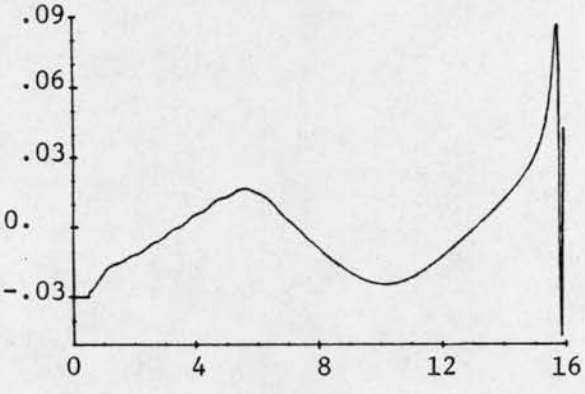

(k) V_{UEL}

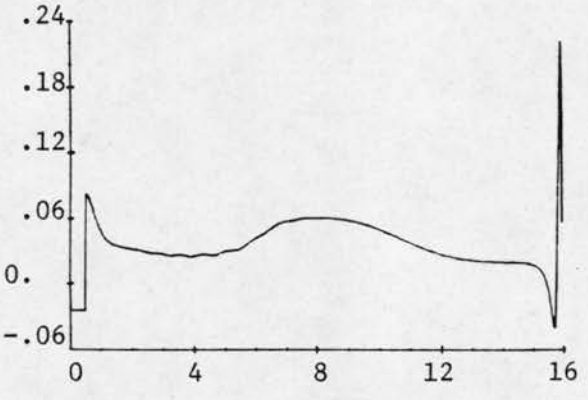

(l) $(V_{UEL}-E)$

Fig. 4.7(cont.) System response with reduced UEL gain. All quantities (p.u.) plotted against time (sec.).

5. CONCLUSIONS AND RECOMMENDATIONS

The initial work clarified the issue of steady-state stability for a single machine infinite bus system. The unregulated round rotor machine was shown to have a region of stability in the PQ plane expressible as a circle. This circle was not derived using traditional approaches such as the classical electromechanical model. The circle was shown to be a description of the locus of points where the field flux mode eigenvalue became zero when all other fast variables were replaced with their slow manifolds. This derivation gives a rigorous explanation of the source of the steady-state stability circle from the dynamic equations of the machine.

During the initial work, the traditional concept of an infinite bus was also clarified. The infinite bus was considered to be a fixed voltage, fixed frequency source only during transients. As various equilibria were considered, the value of the infinite bus was changed. Thus, the infinite bus represents a source which has super slow dynamics. That is, its value changes with load as a model of the external network, but is considered fixed during a given fast transient. While this is a realistic practical representation, it is also necessary if various loading conditions are to be considered at a given value of machine terminal voltage magnitude. That is, it is not possible to independently specify terminal voltage, input P-Q and infinite bus voltage. Since the desired stability circle was specified at unity terminal voltage, this requires different infinite bus voltages for different P-Q loading.

A closed form expression for the SSSL of a fixed excitation synchronous machine was presented in Chapter 2. It might be beneficial to extend this to multimachine systems. Of course, simple results, as in the single machine case, cannot be anticipated. Nevertheless, the use of exact methods of analysis

available at present could lead to observations and conclusions far removed from classical thinking on stability.

The effect of the AVR on machine stability was dealt with in Chapter 3 with a specific example. The stable region may vary depending on the type of excitation system as well as its parameters. It is felt that further insight regarding stability of regulated systems would be of great value.

In Chapter 3, the underexcitation limiter was investigated to determine its impact on stability both in steady state and during transients. The relevance of damping feedback V_F and gain K_{UL} with regard to stability were dealt with in Chapter 4. These parameters were found to be critical. Future work is needed to determine optimal settings for classes of contingencies. UEL dynamics could certainly bring in additional factors to be considered. The optimal setting of UEL parameters would guarantee that the UEL would prevent the machine from entering the unstable regions during slow changes in equilibria, and would also respond during reactive transients to maintain stable operation. The transient analysis would have to be coordinated with other control and protective devices, such as the loss of field relay. The UEL would have to limit underexcitation fast enough so that the loss of field (LOF) relay would not trip the unit unless the UEL, AVR or exciter failed. This coordination would require a study of the dynamics of the LOF relay.

REFERENCES

[1] J. Y. Jackson, "Interpretation and use of generator reactive capability diagrams," IEEE Trans. Industry General Applications, vol. IGA-7, no. 6, Nov./Dec. 1971, pp. 729-732.

[2] E. W. Kimbark, Power System Stability: Synchronous Machines. New York: Dover Publications Inc., 1956.

[3] C. G. Adams and J. B. McClure, "Underexcited operation of turbogenerators," AIEE Trans., vol. 67, 1948, pp. 521-526.

[4] A. S. Rubenstein and M. Temoshok, "Underexcited reactive ampere limit for modern amplidyne voltage regulator," AIEE Trans., vol. 73, 1954, pp. 1433-1438.

[5] T. J. Dutkiewicz and P. A. Fedora, "Operation of generator minimum excitation limiters during islanding, Proc. of the American Power Conference, 1983, vol. 45, pp. 503-508.

[6] P. W. Sauer and M. A. Pai, "Power system dynamics and stability," Unpublished course notes for EE497SP, University of Illinois at Champaign-Urbana, Fall 1984.

[7] Computer Representation of Excitation Systems - IEEE Committee Report, IEEE Trans. Power Apparatus Syst., vol. PAS-87, no. 6 1968, pp. 1460-1464.

APPENDIX A

DERIVATION OF CLASSICAL STABILITY REGION

The derivation of the circle (Equation (1.5)) from purely algebraic considerations is presented here.

Assume the second machine of the two-machine system of Figure 1.3 to be an infinite bus $V\underline{/0}$ in series with an equivalent system reactance jx_e. From classical stability criteria, pullout occurs when the phase angle of $\overline{E}_1$ becomes 90°. Hence at pullout,

$$\overline{E}_1 = E_1\underline{/90} = jE_1 \tag{A.1}$$

Equation (1.3) becomes

$$\overline{I} = \frac{jE_1 - \overline{E}_T}{jx_{d1}} \tag{A.2}$$

and Equation (1.4) becomes

$$\overline{S} = P + jQ = \overline{E}_T \frac{jE_1 - \overline{E}_T}{jx_{d1}}^* \tag{A.3}$$

Or

$$\overline{S} = \frac{E_1\overline{E}_T}{x_{d1}} - j\frac{E_t^2}{x_{d1}} \tag{A.4}$$

where

$$\overline{E}_T = E_t\, e^{j\theta} \tag{A.5}$$

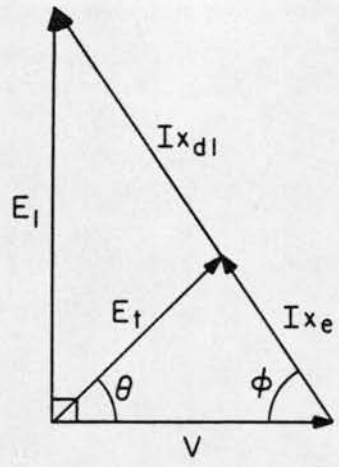

Figure A.1. Phasor diagram of the system at pullout.

From the phasor diagram A.1

$$\frac{E_l}{\sin \phi} = \frac{(x_{dl} + x_e)I}{\sin 90^\circ} \tag{A.6}$$

and

$$\frac{E_t}{\sin \phi} = \frac{x_e I}{\sin \theta} \tag{A.7}$$

Combining (A.5) and (A.6)

$$E_l = \frac{x_{dl} + x_e}{x_e} E_t \sin \theta \tag{A.8}$$

From Equations (A.4) and (A.5),

$$S = \frac{E_1 E_t \cos \theta}{x_{d1}} + j\left[\frac{E_1 E_t \sin \theta}{x_{d1}} - \frac{E_t^2}{x_{d1}}\right] \tag{A.9}$$

Substituting (A.8) into (A.9)

$$P = \frac{x_{d1} + x_e}{x_{d1} + x_e} E_t^2 \sin \theta \cos \theta \tag{A.10}$$

$$Q = \frac{x_{d1} + x_e}{x_{d1} x_e} E_t^2 \sin^2 \theta - \frac{E_t^2}{x_{d1}} \tag{A.11}$$

Now $\sin^2 \theta = (1 - \cos 2\theta)/2$. Hence Equation (A.11) becomes

$$Q = \frac{x_{d1} - x_e}{2x_{d1} x_e} E_t^2 - \frac{x_{d1} + x_e}{2x_{d1} x_e} E_t^2 \cos 2\theta \tag{A.12}$$

From Equations (A.10) and (A.12)

$$P^2 + \left(Q - \frac{x_{d1} - x_e}{2x_{d1} x_e} E_t^2\right)^2 = \left(\frac{x_{d1} + x_e}{2x_{d1} x_e} E_t^2\right)^2 \quad (\sin^2 2\theta + \cos^2 2\theta) \tag{A.13}$$

Or

$$P^2 + \left(Q - \frac{x_{d1} - x_e}{2x_{d1} x_e} E_t^2\right)^2 = \left(\frac{x_{d1} + x_e}{2x_{d1} x_e} E_t^2\right)^2 \tag{A.14}$$

This is the equation of the circle representing SSSL of a synchronous machine. Note that the stability criterion $\delta = 90°$ has been used in the derivation.

APPENDIX B

SYSTEM STABILITY MATRICES

In this section, the linearized stability matrices for the various system models used in Chapter 2 and Chapter 3 are presented. These can be used directly for eigenvalue analysis.

B.1. Sixth Order Model

Linearizing the sixth order machine model given by Equations (2.1) to (2.6) yields the following matrix.

$$
\begin{bmatrix}
-\frac{(r_s + r_e)\,\omega_s}{(x'_d + x_e)} & \omega_s & \frac{(r_s + r_e)\,\omega_s}{(x'_d + x_e)} & 0 & \sqrt{3}\,V^o_\infty\,\omega_s \cos\delta^o & \omega_s \lambda^o_q \\
-\omega_s & -\frac{\omega_s(r_s + r_e)}{(x'_q + x_e)} & 0 & -\frac{\omega_s(r_s + r_e)}{(x'_q + x_e)} & -\sqrt{3}\,V^o_\infty\,\omega_s \sin\delta^o & -\omega_s \lambda^o_d \\
\frac{(x_d - x'_d)}{T'_{do}(x'_d + x_e)} & 0 & -\frac{(x_d + x_e)}{T'_{do}(x'_d + x_e)} & 0 & 0 & 0 \\
0 & \frac{x'_q - x_q}{T'_{qo}(x'_q + x_e)} & 0 & -\frac{(x_q + x_e)}{T'_{qo}(x'_q + x_e)} & 0 & 0 \\
0 & 0 & 0 & 0 & 0 & \omega_s \\
\frac{i^o_q - \lambda^o_q / x'_d + x_e}{6H} & \frac{\lambda^o_d / x'_q + x_e - i^o_d}{6H} & \frac{\lambda^o_q}{6H(x'_d + x_e)} & \frac{\lambda^o_d}{6H(x'_q + x_e)} & 0 & -D'/2H
\end{bmatrix}
$$

$$i_q^o = \lambda_q^o/(x_q + x_e) \tag{B.1}$$

$$i_d^o = \frac{\lambda_d^o - E_q'^o}{(x_d' + x_e)} \tag{B.2}$$

B.2. Fourth Order Model (Equations (2.30) to (2.33))

$$\begin{bmatrix} \frac{-(x_d + x_e)}{T_{do}'(x_d' + x_e)} & 0 & \frac{(x_d' - x_d)\sqrt{3}\, V_\infty^o \sin\delta^o}{T_{do}'(x_d' + x_e)} & 0 \\ 0 & \frac{-(x_q + x_e)}{T_{qo}'(x_q' + x_e)} & \frac{(x_q - x_q')\sqrt{3}\, V_\infty^o \cos\delta^o}{T_{qo}'(x_q' + x_e)} & 0 \\ 0 & 0 & 0 & \omega_s \\ \frac{-V_\infty^o \sin\delta^o}{2H\sqrt{3}(x_d' + x_e)} & \frac{V_\infty^o \cos\delta^o}{2H\sqrt{3}(x_q' + x_e)} & A_{14} & -D'/2H \end{bmatrix}$$

$$A_{14} = -\frac{E_q'^o V_\infty^o \cos\delta^o}{2H\sqrt{3}(x_d' + x_e)} - \frac{E_d'^o V_\infty^o \sin\delta^o}{2H\sqrt{3}(x_q' + x_e)} - (x_d' - x_q')\, V_\infty^o \cos 2\delta^o / 2H(x_d + x_e)(x_q + x_e) \tag{B.3}$$

B.3. Third Order (Flux Decay) Model (Equations (2.34) to (2.36))

$$\begin{pmatrix} \dfrac{-(x_d + x_e)}{T'_{do}(x'_d + x_e)} & \dfrac{(x'_d - x_d)\sqrt{3}\, V^o_\infty \sin \delta^o}{T'_{do}(x'_d + x_e)} & 0 \\ 0 & 0 & \omega_s \\ \dfrac{-V^o_\infty \sin \delta^o}{2H\sqrt{3}(x'_d + x_e)} & \dfrac{-V^o_\infty E'^o_q \cos \delta^o}{2H\sqrt{3}(x'_d + x_e)} & -D'/2H \\ & + \dfrac{(x_q - x'_d)\, V^{o2}_\infty \cos 2\delta^o}{2H(x'_d + x_e)(x_q + x_e)} & \end{pmatrix}$$

B.4. Second Order (Constant E'_q) Model (Equations (2.37), (2.38)

$$\begin{bmatrix} 0 & \omega_s \\ \dfrac{-V^o_\infty E'^o_q \cos \delta^o}{2H\sqrt{3}(x'_d + x_e)} & -D'/2H \\ + \dfrac{(x_q - x'_d)\, V^{o2}_\infty \cos 2\delta^o}{2H\sqrt{3}(x_q + x_e)(x'_d + x_e)} & \end{bmatrix}$$

B.5. Second Order (Constant E'_q, Constant E'_d) Model (Equations (2.39), (2.40))

$$\begin{bmatrix} 0 & \omega_s \\ A_{14} & -D'/2H \end{bmatrix}$$

A_{14} is given in Equation (B.3).

B.6. System Model with AVR (Equations (2.34) to (2.36), (3.1) to (3.4))

$$\begin{bmatrix}
-\frac{1}{T'_{do}}\frac{x_d + x_e}{x'_d + x_e} & -\frac{1}{T'_{do}}\frac{x_d - x'_d}{x'_d + x_e}\sqrt{3}\,V^o_\infty \sin\delta^o & 0 & \frac{\sqrt{3}}{T'_{do}} & 0 & 0 \\
0 & 0 & \omega_s & 0 & 0 & 0 \\
-\frac{V^o_\infty \sin\delta^o}{2\sqrt{3}H(x'_d + x_e)} & -\frac{V^o_\infty E^o_q \cos\delta^o}{2\sqrt{3}H(x'_d + x_e)} & 0 & 0 & 0 & 0 \\
 & -\frac{V^o_\infty \cos 2\delta^o}{2H}\left[\frac{1}{x_q + x_e} - \frac{1}{x'_d + x_e}\right] & & & & \\
0 & 0 & 0 & -\frac{K_E + S_E}{T_E} & 0 & \frac{1}{T_E} \\
0 & 0 & 0 & -\frac{K_F(K_E + S_E)}{T_E T_F} & -\frac{1}{T_F} & \frac{K_F}{T_E T_F} \\
-\frac{K_A}{T_A}\frac{x_e V^o_q}{3E_t(x'_d + x_e)} & -\frac{K_A}{T_A}\left[\frac{x_q V^o_d V^o_\infty \cos\delta^o}{\sqrt{3}\,E_t(x_q + x_e)}\right. & 0 & 0 & -\frac{K_A}{T_A} & -\frac{1}{T_A} \\
 & \left. -\frac{x'_d V^o_q V^o_\infty \sin\delta^o}{\sqrt{3}\,E_t(x'_d + x_e)}\right] & & & &
\end{bmatrix}$$

B.7. System Model with UEL Overriding AVR (Equations (3.5) to (3.8), (2.34) to (2.36))

$$
\begin{bmatrix}
-\frac{(x_d + x_e)}{T'_{do}(x'_d + x_e)} & -\frac{\sqrt{3}(x_d - x'_d)\, V^o_\infty \sin\delta^o}{T'_{do}(x'_d + x_e)} & 0 & \frac{\sqrt{3}}{T'_{do}} & 0 & 0 \\
0 & 0 & \omega_s & 0 & 0 & 0 \\
-\frac{V^o_\infty \sin\delta^o}{2\sqrt{3}H(x'_d + x_e)} & -\frac{V^o_\infty E'^o_q \cos\delta^o}{2\sqrt{3}H(x'_d + x_e)} & 0 & 0 & 0 & 0 \\
 & -\frac{(x'_d - x_q)\, V^{o2}_\infty \cos 2\delta^o}{2H(x_q + x_e)(x'_d + x_e)} & & & & \\
0 & 0 & 0 & -\left(\frac{K_E + S_E}{T_E}\right) & 0 & \frac{1}{T_E} \\
0 & 0 & 0 & -\frac{K_F(K_E + S_E)}{T_E T_F} & -\frac{1}{T_F} & \frac{K_F}{T_E T_F} \\
\frac{K_A}{T_A} K_{UL} B' & \frac{K_A}{T_A} K_{UL} A' & 0 & 0 & -\frac{K_A K_{UL} K_{FL}}{T_A} & -\frac{1}{T_A}
\end{bmatrix}
$$

The relevant equations are given below.

$$A' = \frac{\alpha_o a_1 + \beta_o a_2}{\sqrt{3}\sqrt{\alpha_o^2 + \beta_o^2}} - \frac{K_r(AV^o_d + BV^o_q)}{3E_t} \qquad (B.5)$$

$$B' = \frac{\alpha_o b_1 + \beta_o b_2}{\sqrt{3}\sqrt{\alpha_o^2 + \beta_o^2}} - \frac{K_R C V^o_q}{3E_t} \qquad (B.6)$$

$$V_d^o = \frac{x_q}{x_q + x_e} \sqrt{3}\, V_\infty^o \sin \delta^o \tag{B.7}$$

$$V_q^o = \frac{x_e}{x_d' + x_e} E_q'^o + \frac{x_d'}{x_d' + x_e} \sqrt{3}\, V_\infty^o \cos \delta^o \tag{B.8}$$

$$I_d^o = \frac{\sqrt{3}\, V_\infty^o \cos \delta^o - E_q'^o}{x_d' + x_e} \tag{B.9}$$

$$I_q^o = - \frac{\sqrt{3}\, V_\infty^o \sin \delta^o}{x_q + x_e} \tag{B.10}$$

$$A = \frac{x_q}{x_q + x_e} \sqrt{3}\, V_\infty^o \cos \delta^o \tag{B.11}$$

$$B = - \frac{x_d'}{x_d' + x_e} \sqrt{3}\, V_\infty^o \sin \delta^o \tag{B.12}$$

$$C = \frac{x_e}{x_d' + x_e} \tag{B.13}$$

$$D = - \frac{\sqrt{3}\, V_\infty^o \sin \delta_o}{x_d' + x_e} \tag{B.14}$$

$$E = - \frac{1}{x_d' + x_e} \tag{B.15}$$

$$F = - \frac{\sqrt{3}\, V_\infty^o \cos \delta^o}{x_q + x_e} \tag{B.16}$$

$$\alpha_o = (K_C V_d^o - K_I I_q^o) \sin \delta_o + (K_c V_q^o + K_I I_d^o) \cos \delta_o \tag{B.17}$$

$$\beta_o = (K_C V_q^o + K_I I_d^o) \sin \delta^o + (K_I I_q^o - K_c V_d^o) \cos \delta^o \quad \text{(B.18)}$$

$$a_1 = [K_C(V_d^o + B) + K_I(D - I_q^o)] \cos \delta^o + [K_C(A - V_q^o) - K_I(F + I_d^o)] \sin \delta^o \quad \text{(B.19)}$$

$$b_1 = [K_C C + K_I E] \cos \delta^o \quad \text{(B.20)}$$

$$a_2 = [K_C(V_q^o - A) + K_I(I_d^o + F)] \cos \delta^o + [K_C(V_d^o + B) + K_I(D - I_q^o)] \sin \delta^o \quad \text{(B.21)}$$

$$b_2 = [K_C C + K_I E] \sin \delta^o \quad \text{(B.22)}$$

APPENDIX C

PROGRAM LISTINGS

The following FORTRAN listings are given in the forthcoming pages.

1. SSSL of an unregulated machine for sixth order model.
2. SSSL of a regulated machine with IEEE Type 1 excitation system.
3. Simulation of reaction transients in a regulated machine.

All the programs have been written for use on the CDC Cyber 175 computer.

```
C    THIS PROGRAM EVALUATES THE SSSL OF A FIXED EXCITATION
C    SYNCHRONOUS MACHINE, USING A SIXTH ORDER MODEL. WITH
C    THE STABILITY MATRIX SUITABLY MODIFIED (REFER TO APPENDIX
C    A), THE PROGRAM CAN BE USED FOR OTHER MODELS.
C
         PROGRAM STAB6 (INPUT,OUTPUT,DAT,RES,TAPE7=DAT,TAPE8=RES)
         REAL A(6,6),Z(6,6),WR(6),WI(6),FV1(6),WRP(6),WIP(6)
         INTEGER IV1(6)
         COMPLEX PWR,CURNT,E,V,VT,S,ZE,D,AIDQ,SHIFT
C
         READ(7,50) XE,XD,XQ,XDPR,XQPR
         READ(7,50) OM,H,TDO,TQO,DPR
         READ(7,60) VT
         SQ = SQRT(3.0)
         DO 99 K = 1,22
         READ(7,55) P,Q,QDEL,XMD
         VOLT = 0.0
         DELTA = 0.0
         VINF = 0.0
         NM = 6
         N = NM
C    WR(N) & WI(N) CONTAIN THE REAL AND IMAGINARY PARTS OF
C    THE EIGENVALUES.
         DO 1 I = 1,N
         WR(I) = 0.0
         WI(I) = 0.0
1        CONTINUE
C    A(N,N) IS THE SYSTEM STABILITY MATRIX.
5        DO 10 I =1,N
         DO 10 J =1,N
         A(I,J) = 0.0
10       CONTINUE
         A(1,2) = OM
         A(2,1) = -OM
         A(3,1) = (XD-XDPR)/(TDO*(XE+XDPR))
         A(4,2) = (XQPR-XQ)/(TQO*(XE+XQPR))
         A(3,3) = -(XE+XD)/(TDO*(XE+XDPR))
         A(4,4) = -(XE+XQ)/(TQO*(XE+XQPR))
         A(5,6) = OM
         A(6,6) =-DPR/(2.0*H)
         DELP = DELTA
         VOLP = VOLT
         VINFP = VINF
         DO 15 I=1,N
         WRP(I) = WR(I)
         WIP(I) = WI(I)
15       CONTINUE
C
C    CALCULATION OF THE EQUILIBRIUM POINT.
         PWR = CMPLX(P,Q)
         CURNT = CONJG(PWR/VT)
         ZE = CMPLX(0.0,XE)
         V = VT+ZE*CURNT
         VINF = CABS(V)
         THETA = CARG(V)
         SHIFT = CMPLX(COS(THETA),-SIN(THETA))
```

```
      VT = VT*SHIFT
      CURNT = CURNT*SHIFT
      S = CMPLX(0.0,XQ)
      E = VT-S*CURNT
      VOLT = CABS(VT)
      DELTA = CARG(E)
      DR = SQ*SIN(DELTA)
      DI = SQ*COS(DELTA)
      D = CMPLX(DR,DI)
      AIDQ = D*CURNT
      R = REAL(AIDQ)
      FCRNT = (SQ*CABS(E)-(XD-XQ)*R)/XMD
      FLUXD = (XD+XE)*R+XMD*FCRNT
      FLUXQ = (XQ+XE)*AIMAG(AIDQ)
      EQPR = FLUXD-(XDPR+XE)*R
      EDPR = -FLUXQ+(XQPR+XE)*AIMAG(AIDQ)
C
      A(1,5) = SQ*OM*COS(DELTA)*VINF
      A(1,6) = OM*FLUXQ
      A(2,5) = -SQ*OM*SIN(DELTA)*VINF
      A(2,6) = -OM*FLUXD
      A(6,1) = (AIMAG(AIDQ)-FLUXQ/(XE+XDPR))/(6.0*H)
      A(6,2) = (FLUXD/(XE+XQPR)-R)/(6.0*H)
      A(6,3) = FLUXQ/(6.0*H*(XE+XDPR))
      A(6,4) = FLUXD/(6.0*H*(XE+XQPR))
C   A LIBRARY ROUTINE IS USED TO CALCULATE EIGENVALUES.
      MATZ = 0.0
      CALL RG(NM,N,A,WR,WI,MATZ,Z,IV1,FV1,IERR)
      Q = Q+QDEL
C   CHECKING FOR INSTABILITY.
      DO 20 I = 1,N
      IF((WR(I).GT.0.0).AND.(ABS(WI(I)).LT.375.0)) GO TO 25
20    CONTINUE
C   IF STABLE, THE ABOVE PROCEDURE IS REPEATED AFTER
C   SUITABLY ALTERING Q.
      GO TO 5
C
25    WRITE(8,30) VOLP,DELP,VINFP
      QP = Q-2.0*QDEL
      WRITE(8,35)P,QP
      WRITE(8,40) (WRP(I),I=1,N)
      WRITE(8,40) (WIP(I),I=1,N)
      WRITE(8,30) VOLT,DELTA,VINF
      WRITE(8,35) PWR
      WRITE(8,40) (WR(I),I=1,N)
      WRITE(8,40) (WI(I),I=1,N)
      WRITE(8,45)
C   OUTER LOOP TO VARY P.
99    CONTINUE
30    FORMAT('VOLT =',F9.5,'/','DELTA =',F9.5,'/','VINF =',F9.5,/)
35    FORMAT('POWER =',2F10.5,/)
40    FORMAT(6F12.6,/)
45    FORMAT(80('-'))
50    FORMAT(5F10.5)
55    FORMAT(4F10.5)
60    FORMAT(2F10.5)
```

```
      STOP
      END
C
C   CALCULATION OF ARGUMENT OF A COMPLEX NUMBER.
      FUNCTION CARG(X)
      COMPLEX X
      X1 = REAL(X)
      X2 = AIMAG(X)
      ZER = 1.0E-99
      IF(ABS(X).LE.ZER) GO TO 10
      CARG = ATAN2(X2,X1)
      RETURN
10    IF(X2.LT.0.0) GO TO 30
      IF(X2.GT.0.0) GO TO 20
      CARG = 0.0
      RETURN
20    CARG = 2.0*ATAN(1.0)
      RETURN
30    CARG = -2.0*ATAN(1.0)
      RETURN
      END
```

```
C    THIS PROGRAM EVALUATES THE STEADY-STATE STABILITY LIMIT OF A
C    REGULATED MACHINE IN THE P-Q PLANE. AN IEEE TYPE 1 EXCITATION
C    SYSTEM IS USED WITH THE FLUX DECAY MODEL FOR THE MACHINE.
C
         PROGRAM AVR (INPUT,OUTPUT,DAT,DUE,TAPE7=DAT,TAPE8=DUE)
         REAL A(6,6),Z(6,6),WR(6),WI(6),EV1(6),WRP(6),WIP(6)
         INTEGER IV1(6)
         COMPLEX PWR,CURNT,E,V,VT,S,ZE,D,AIDQ,SHIFT,ALFA,VDQ
C
         READ(7,50) XE,XD,XQ,XDPR,XQPR
         READ(7,50) OM,H,TDO,AKF,TF
         READ(7,50) AKE,TE,SE,AKA,TA
         DO 99 K = 1,20
         READ(7,50) VT,P,Q,QUIL
         SQ = SQRT(3.0)
         NM = 6
         N = NM
         DO 1 I = 1,N
         WR(I) = 0.0
         WI(I) = 0.0
1        CONTINUE
C    A(N,N) IS THE STABILITY MATRIX OF THE SYSTEM.
5        DO 10 I =1,N
         DO 10 J =1,N
         A(I,J) = 0.0
10       CONTINUE
         DO 7 I = 1,N
         WRP(I) = WR(I)
         WIP(I) = WI(I)
7        CONTINUE
C
         A(1,1) = -(XD+XE)/((XDPR+XE)*TDO)
         A(1,4) = SQ/TDO
         A(2,3) = OM
         A(4,4) = -(AKE+SE)/TE
         A(4,6) = 1.0/TE
         A(5,4) = -AKF*(AKE+SE)/(TE*TF)
         A(5,5) = -1.0/TF
         A(5,6) = AKF/(TE*TF)
         A(6,5) = -AKA/TA
         A(6,6) = -1.0/TA
C
C    CALCULATION OF EQUILIBRIUM VALUES OF RELEVANT VARIABLES.
         PWR =CMPLX(P,Q)
         CURNT = CONJG(PWR/VT)
         ZE = CMPLX(0.0,XE)
         V = VT+ZE*CURNT
         VINF = CABS(V)
         THETA = CARG(V)
         SHIFT = CMPLX(COS(THETA),-SIN(THETA))
         VT = VT*SHIFT
         CURNT = CURNT*SHIFT
         S = CMPLX(0.0,XQ)
         E = VT-S*CURNT
         VOLT = CABS(VT)
         DELTA = CARG(E)
```

```
      DR = SQ*SIN(DELTA)
      DI = SQ*COS(DELTA)
      D = CMPLX(DR,DI)
      AIDQ = D*CURNT
      EQPR = SQ*VINF*COS(DELTA)-(XDPR+XE)*REAL(AIDQ)
      VD = XQ*SQ*VINF*SIN(DELTA)/(XQ+XE)
      VQ = (XE*EQPR+SQ*XDPR*VINF*COS(DELTA))/(XDPR+XE)
      VDQ = CMPLX(VD,VQ)
      EX = ((XD+XE)*EQPR/SQ-(XD-XDPR)*VINF*COS(DELTA))
      EX = EX/(XDPR+XE)
      VR = EX*(AKE+SE)
C
      A(1,2) = -SQ*VINF*(XD-XDPR)*SIN(DELTA)/((XDPR+XE)*TDO)
      A(3,1) = -VINF*SIN(DELTA)/(2.0*H*SQ*(XDPR+XE))
      A321 = VINF*EQPR*COS(DELTA)/(2.0*SQ*H*(XDPR+XE))
      A322 = VINF*VINF*COS(2.0*DELTA)*(XDPR-XQ)/(2.0*H*(XQ+XE))
      A(3,2) = -(A321+A322/(XDPR+XE))
      A(6,1) = -AKA*XE*AIMAG(VDQ)/(CABS(VT)*(XDPR+XE)*3.0*TA)
      C1 = VD*SQ*XQ*VINF*COS(DELTA)/(3.0*CABS(VT)*(XQ+XE))
      C2 = VQ*SQ*XDPR*VINF*SIN(DELTA)/(3.0*(XDPR+XE)*CABS(VT))
      A(6,2) = -AKA*(C1-C2)/TA
C
C   A LIBRARY ROUTINE RG IS CALLED TO CALCULATE EIGENVALUES.
      MATZ = 0.0
      CALL RG(NM,N,A,WR,WI,MATZ,Z,IV1,FV1,IERR)
C   CHECKING FOR INSTABILITY.
      DO 20 J = 1,N
      IF(WR(J).GT.0.0) GO TO 25
20    CONTINUE
C   IF STABLE  Q IS ALTERED  AND THE ABOVE PROCEDURE IS
C   REPEATED UNTIL STABILITY LIMIT IS REACHED FOR A GIVEN
C   VALUE OF P.
      Q = Q + QDEL
      GO TO 5
C
25    WRITE(8,30) VOLT,DELTA,VINF
      WRITE(8,65) EQPR,EX,VR
      WRITE(8,35) PWR
      WRITE(8,40) (WRP(I),I = 1,N)
      WRITE(8,40) (WIP(I),I = 1,N)
      WRITE(8,40) (WR(I),I=1,N)
      WRITE(8,40) (WI(I),I=1,N)
      WRITE(8,45)
C   DO LOOP FOR VARYING P.
99    CONTINUE
30    FORMAT('VOLT =',F9.5,'/','DELTA =',F9.5,'/','VINF =',F9.5,/)
35    FORMAT('POWER =',2F10.5,/)
40    FORMAT(6F12.6,/)
45    FORMAT(80('-'))
50    FORMAT(5F10.5)
55    FORMAT(4F10.5)
60    FORMAT(2F10.5)
65    FORMAT('EQPR =',F10.5,'/','EX =',F10.5,'/','VR =',F10.5)
      STOP
      END
```

```
C   FUNCTION SUBROUTINE TO EVALUATE ARGUMENT OF A COMPLEX NO.
      FUNCTION CARG(X)
      COMPLEX X
      X1 = REAL(X)
      X2 = AIMAG(X)
      ZER = 1.0E-99
      IF(ABS(X).LE.ZER) GO TO 10
      CARG = ATAN2(X2,X1)
      RETURN
10    IF(X2.LT.0.0) GO TO 30
      IF(X2.GT.0.0) GO TO 20
      CARG = 0.0
      RETURN
20    CARG = 2.0*ATAN(1.0)
      RETURN
30    CARG = -2.0*ATAN(1.0)
      RETURN
      END
```

```
C    SIMULATION OF REACTIVE TRANSIENTS IN A REGULATED MACHINE.
C    SYSTEM MODEL. - FLUX DECAY MODEL FOR MACHINE;IEEE TYPE1
C    EXCITATION SYSTEM, MODIFIED TO INCLUDE A UEL.
C
         PROGRAM MEL(INPUT,OUTPUT,GIV,TIC,TOC,TAPE7=GIV,TAPE8=TOC,
     $ TAPE2=TIC)
         DIMENSION C(24),W(6,9),Y(6),YPRIME(6)
         EXTERNAL FCN
         COMPLEX PWR,VTERM,AIT,SHUNT,PINF,VINF,AIDQ,U,E,D,Z,ZE
         COMMON TSW,TM,XD,XQ,XE,XDPR,TDPR,H,AKC,AKI,AKR,AKUL,TE,AKE,SE,TF,
     $ AKF,TA,AKA,V0,V01,XE1,VREF,PWR,VT,E1,E2,IND1,IND2,Y4Z
C
         N = 6
         NW = N
         TOL = .01
         IND = 1
C    SYSTEM RESPONSE UPTO TSTOP SEC. IS EVALUATED IN STEPS OF
C    TSTEP SEC.
         TSTOP = 20.00
         TSTEP = 0.020
         TEND = 0.0
C    TSW. IS THE INSTANT AT WHICH THE TRANSIENT IS INITIATED.
         TSW = 0.5
         T = 0.
         E1 = 0.0
         E2 = 0.0
C
         READ(7,30) XD,XQ,XDPR,XE,XL,H,TDPR
         READ(7,30) AKUL,AKR,AKI,AKC,AKE,TE,SE
         READ(7,30) AKA,TA,AKF,TF,VT,P,Q
         READ(7,50) IND1,IND2
C
C    CALCULATION OF INITIAL EQUILIBRIUM-Y(I) ARE THE STATES.
         PWR = CMPLX(P,Q)
         VTERM = CMPLX(VT,0.0)
         AIT = CONJG(PWR/VTERM)
         XE1 = XE
         XE = XE*XL/(XL+XE)
         ZE = CMPLX(0.0,XE)
         VINF = VTERM+ZE*AIT
         PHI = CARG(VINF)
         U = CMPLX(COS(PHI),-SIN(PHI))
         VTERM = VTERM*U
         AIT = CONJG(PWR/VTERM)
         V0 = CABS(VINF)
         V01 = V0*(XL+XE1)/XL
         Z = CMPLX(0.0,XQ)
         E = VTERM-Z*AIT
         Y(2) = CARG(E)
         SQ = SQRT(3.0)
         DR = SQ*SIN(Y(2))
         DI = SQ*COS(Y(2))
         D = CMPLX(DR,DI)
         AIDQ = D*AIT
         Y(1) = SQ*V0*COS(Y(2))-(XDPR+XE)*REAL(AIDQ)
```

```
      Y(3) = 1.0
      TM = -P
      Y(4) = ((XD+XE)*Y(1)/SQ-(XD-XDPR)*VO*COS(Y(2)))/(XDPR+XE)
      Y4Z = Y(4)
      Y(5) = 0.0
      Y(6) = Y(4)*(AKE+SE)
      EFR = Y(6)/AKA
      VREF = EFR+VT+Y(5)
10    P = REAL(PWR)
      Q = AIMAG(PWR)
C
C   LIMITS FOR REGULATOR AMPLIFIER.
      IF(Y(6).GT.2.1) Y(6) = 2.1
      IF(Y(6).LT.-1.0)Y(6) = -1.0
      E3 = E2-E1
      WRITE(8,15) T,P,Q,VT,(Y(I),I = 1,N)
15    FORMAT(1X,10E11.4)
      WREL = Y(3)-1.0
      WRITE(2,40) T,E1,E2,E3,WREL
      TEND = TEND+TSTEP
      IF(TEND.GT.TSTOP) GO TO 25
C LIBRARY ROUTINE FOR INTEGRATION.
      CALL DVERK (N,FCN,T,Y,TEND,TOL,IND,C,NW,W,IER)
      IF(IND.NE.3) WRITE(6,20) IND
20    FORMAT('ERROR CODE IND = ',I5)
      T = TEND
      GO TO 10
25    CONTINUE
30    FORMAT(7F10.5)
40    FORMAT(1X,7E11.4)
50    FORMAT(2I2)
      STOP
      END
C
C   SUBROUTINE FOR EVALUATING DERIVATIVES OF Y(I).
C   CALLED FROM INTEGRATION ROUTINE.
      SUBROUTINE FCN (N,T,Y,YPRIME)
      REAL Y(N),YPRIME(N)
      COMPLEX VTERM,VINF,AIDQ,AIT,X,X1,ZE,PWR,D,E
      COMMON TSW,TM,XD,XQ,XE,XDPR,TDPR,H,AKC,AKI,AKR,AKUL,TE,AKE,SE,TF,
     $ AKF,TA,AKA,VO,VO1,XE1,VREF,PWR,VT,E1,E2,IND1,IND2,Y4Z
C   CONTROL STATEMENT FOR SWITCHING.
      IF(T.LT.TSW) GO TO 50
      VO = VO1
      XE = XE1
50    YP11 = -Y(1)*(XD+XE)/(XDPR+XE)
      YP12 = (XD-XDPR)*SQRT(3.0)*VO*COS(Y(2))/(XDPR+XE)
      YP13 = SQRT(3.0)*Y(4)
      YPRIME(1) = (YP11+YP12+YP13)/TDPR
      YPRIME(2) = 377.0*(Y(3)-1.0)
      YP31 = VO*Y(1)*SIN(Y(2))/(SQRT(3.0)*(XE+XDPR))
      YP32 = 0.5*VO*VO*SIN(2.0*Y(2))*(XDPR-XQ)/((XQ+XE)*(XDPR+XE))
      YPRIME(3) = (TM-YP31-YP32)/(2.0*H)
      AID = (SQRT(3.0)*VO*COS(Y(2))-Y(1))/(XDPR+XE)
      AIQ = -(SQRT(3.0)*VO*SIN(Y(2)))/(XQ+XE)
```

```
      AIDQ = CMPLX(AID,AIQ)
      XR = SIN(Y(2))/SQRT(3.0)
      XI = -COS(Y(2))/SQRT(3.0)
      X = CMPLX(XR,XI)
      AIT = X*AIDQ
      VINF = CMPLX(V0,0.0)
      ZE = CMPLX(0.0,XE)
      VTERM = VINF-ZE*AIT
      VT = CABS(VTERM)
      E1 = VREF-Y(5)-VT
      X1 = CMPLX(0.0,1.0)
C     BLOCK CALCULATING UEL OUTPUT.
       D = AKC*VTERM+AKI*X1*AIT
       VALU1 = CABS(D)
       E = AKR*VTERM
       VALU2 = CABS(E)
      E2 = AKUL*(VALU1-VALU2-2.0*Y(5))
      EPR = AMAX1(E1,E2)
C     OPTION FOR SIMULATION EXCLUDING UEL.
      IF(IND2.EQ.0) EPR = E1
      PWR = CONJG(AIT)*VTERM
      YPRIME(4) = (Y(6)-(AKE+SE)*Y(4))/TE
      YPRIME(5) = (-Y(5)+AKF*YPRIME(4))/TF
      YPRIME(6) = (-Y(6)+AKA*EPR)/TA
C
C     OPTION FOR SIMULATION OF AN UNREGULATED MACHINE.
      IF(IND1.EQ.1) GO TO 75
      YPRIME(4) = 0.0
      YPRIME(5) = 0.0
      YPRIME(6) = 0.0
75    CONTINUE
      RETURN
      END
C
C     FUNCTION SUBROUTINE FOR COMPLEX NO. ARGUMENTS.
      FUNCTION CARG(X)
      COMPLEX X
      X1 = REAL(X)
      X2 = AIMAG(X)
      ZER = 1.0E-99
      IF(ABS(X).LE.ZER) GO TO 10
      CARG = ATAN2(X2,X1)
      RETURN
10    IF(X2.LT.0.0) GO TO 30
      IF(X2.GT.0.0) GO TO 20
      CARG = 0.0
      RETURN
20    CARG = 2.0*ATAN(1.0)
      RETURN
30    CARG = -2.0*ATAN(1.0)
      RETURN
      END
```